MODIFIED OPW METHOD

A MODIFIED ORTHOGONALIZED PLANE WAVE METHOD FOR THE CALCULATION OF BAND STRUCTURES IN TRANSITION METALS

By

ROSS ALFRED DEEGAN, B.Sc., B.Eng.

A Thesis

Submitted to the Faculty of Graduate Studies

in Partial Fulfilment of the Requirements

for the Degree

Doctor of Philosophy

McMaster University

May 1967

DOCTOR OF PHILOSOPHY (1967) McMASTER UNIVERSITY
(Physics) Hamilton, Ontario.

TITLE: A Modified Orthogonalized Plane Wave Method for the Calculation of Band Structures in Transition Metals.

AUTHOR: Ross Alfred Deegan, B.Sc. (Loyola College)

B.Eng. (McGill University)

SUPERVISOR: Dr. W. D. Twose

NUMBER OF PAGES: vi, 73

SCOPE AND CONTENTS:

This thesis describes some modifications to the orthogonalized plane wave method designed to make the method applicable to calculating the band structure of transition metals. The procedure is to augment the basis set of OPW's by including functions which vanish in the interstitial regions but represent well the outer core functions and the d-band states near the nucleus. The method is applied to the transition metal niobium, with emphasis on the applicability of the procedure. The convergence of the method is discussed and the resulting band structure of niobium is presented.

ACKNOWLEDGEMENTS

I wish to express my appreciation to Dr. W. D. Twose for proposing and supervising this project and for his continued interest and assistance. I would like to thank also Dr. E. J. Woll, Dr. S. H. Vosko, Dr. J. P. Carbotte, Dr. R. A. Moore and Dr. L. M. Falicov for helpful discussions at various stages of this work.

The numerical calculations were performed on the McMaster University IBM 7040 computer. The cooperation of the staff of the computation centre, particularly the availability of the computer library subroutines, is gratefully acknowledged.

I am indebted to the Ontario Government and the National Research Council of Canada for financial assistance in this work.

TABLE OF CONTENTS

LIST OF FIGURES AND TABLES

Table of Contents (cont'd)

INTRODUCTION

Background

The object of a band structure calculation is the theoretical determination of the single particle energies of the electrons in a solid. This involves two main steps: the choice of a realistic one-body crystalline potential and, in the non-relativistic case (which is the only case with which this work in concerned), the solution of Schrödinger's equation for a solid with that potential.

The completely localized, or core levels, of the potential are easily determined by the methods of atomic physics. One method of solution for the band levels is a variational calculation using a complete set of plane waves, $e^{i\vec{k}\cdot\vec{r}}$. Because of the lattice periodicity only those wave vectors which reduce to the $\vec{k}$ value of the desired Bloch state need be included. If the plane waves are orthogonalized to the core levels, and a variational calculation is performed using a limited number of these orthogonalized plane waves (OPW's), then the lowest roots of the secular equation will converge to the lowest band levels as the number of OPW's is increased. This is the orthogonalized plane wave (OPW) method, first proposed by Herring in 1940 (H40). This method is useful if proximity to convergence is reached with a small number

of trial functions.

In 1959 Phillips and Kleinman (PK59) showed that the OPW method is equivalent to solving the Schrödinger equation with an effective state-dependent potential, the pseudopotential, by expanding the solution of the variational calculation in plane waves. If convergence is good in an OPW calculation then the major contribution to the wave function comes from a single OPW. This corresponds to a pseudopotential whose solution is dominated by a single plane wave, that is, a pseudopotential which nearly vanishes. This clarifies the free election type of behavior present in the simple metals, for which the OPW method is successful. The one-OPW approximation is useful because it provides a simple form for the conduction wave functions, which can then be used to calculate many physical properties of the solid (e.g. total binding energy, vibration spectrum, positron annihilation characteristics). The pseudopotential method also permits good approximate calculations of the band structures of simple metals and semi-conductors by adjusting only a few parameters to fit experimental results (such as de Haas-van Alphen data).

Another modified plane wave approach for band structure calculations is the augmented plane wave (APW) method. Here the procedure is to solve exactly for the wave functions in a sphere centred on each lattice point and employ the variational principle with plane waves to construct the wave functions in the interstitial regions.

A band structure calculation should be done self-consistently, that is, the core and conduction states should be the solutions for a potential which is constructed from the wave functions of these states. In practice the difficulty is twofold: first, it is not clear what prescription to use on the wave functions to construct a potential which takes good account of correlation effects; secondly, the computational problem is great since it is necessary to use the wave functions at many points of the Brillouin zone, at each of which they are described by a different combination of a number of trial functions. The first attempt at several iterations was that of Loucks and Cutler in 1964 (LC64) for beryllium, in which the potential was constructed using as conduction wave functions the one-OPW solutions of the preceding potential in the iterative procedure. Golin (G65) performed a more extensive self-consistent OPW calculation for arsenic in 1965. His work also contains a simplified method for handling non-muffin-tin potentials.

Objectives

The convergence of the OPW method has been found to become poorer as the dominant angular momentum component of the band under consideration increases. Accordingly,it has been usefully applied to the s- and p-like bands of metals and semi-conductors but has not been successful (in its

unmodified form) in calculations of d-bands such as occur in transition metals. In the latter cases the difficulty of orthogonalizing to the outermost s and p core states is added to the problem of slow convergence. Neither of these difficulties is restrictive in the APW approach which has been successfully applied to the first transition series (M64).

In comparison with the OPW method the APW approach has some disadvantages: In the variational procedure many radial wave functions must be integrated for each trial energy in solving the secular equation. (It also follows from this that it contains no simple equivalent to the one-OPW approximation.) The trial wave functions have a discontinuous slope at the surface of the APW sphere. Also, APW applications thus far have been restricted to muffin-tin potentials only and with this restriction self-consistency cannot be attained.

The object of the present work is to modify the OPW procedure to permit its application to transition metals while at the same time retaining its advantages in comparison to other methods of band structure computation. The initial aim was to find a simple approximation to the wave functions. (The specific problem at hand was a first principle calculation of phonon dispersion relations in niobium for comparison with experiment. Such calculations for simple metals have made use of the one-OPW approximation.) The specific topic

of this thesis is the design and application of suitable modifications to the OPW approach. The emphasis in this work has been on the development of the method.

In the first chapter the OPW and APW methods will be reviewed. The following chapter will contain a description of modifications to the OPW method. The application of the modified method to the transition metal niobium and the resultant band structure will then be presented.

CHAPTER I

STANDARD PLANE WAVE METHODS

OPW Method

The requirement is to solve Schrodinger's equation

$$H|\psi\rangle = E|\psi\rangle \qquad (1\text{-}1)$$

for the conduction wave functions ψ, where the one electron Hamiltonian in atomic units is

$$H = -\nabla^2 + V(\vec{r}). \qquad (1\text{-}2)$$

(A word first on notation: ψ will always denote a solution of (1-1) and the trial functions to be used in a variational calculation will be denoted by ϕ. Radial wave functions will be designated $R_{n\ell}(r)$, while the term 'radial wave function' will also be used loosely to mean $P_{n\ell}(r) = rR_{n\ell}(r)$; which of the two is meant will always be clear from the context or from the R-P notation. By 'core states' will be meant the completely localized solutions of (1-1) with the crystalline potential which is to be used to determine the conduction states*.)

---

*Elsewhere these are sometimes called pseudo-core states since they differ from the true core states of the solid. The latter represent the true charge distribution near the core and are the solutions of a different one-body potential.

The potential is periodic in the lattice

$$V(\vec{r}+\vec{R}_\ell) = V(\vec{r}) \qquad (1\text{-}3)$$

for all lattice vectors $\vec{R}_\ell$. In the following discussion the solid will be assumed to have a Bravais lattice structure. By the Bloch theorem the solutions will be of the form

$$\psi_k(\vec{r}) = e^{i\vec{k}\cdot\vec{r}}\, u_k(\vec{r}) \qquad (1\text{-}4)$$

where $u_k(\vec{r})$ is periodic in the lattice. It follows directly that for any functions of this form

$$\langle\psi_{k'}|H|\psi_k\rangle = \langle\psi_{k'}|\psi_k\rangle = 0 \text{ for } \vec{k}' \neq \vec{k}+\vec{G} \qquad (1\text{-}5)$$

for some reciprocal lattice vector $\vec{G}$ (including the zero vector), where the matrix element implies integration over the entire crystal.

The contributions to the matrix element of the Hamiltonian (or unity) from each cell in direct space are equal. This is easily shown as follows: Let $\int^1$ denote the integral in which $\vec{r}$ varies over one cell centred at $\vec{r} = \vec{R}_\ell$ and $\int$ denote the integral with $\vec{r}$ varying over one cell centred at $\vec{r}=o$. Then the contribution to the matrix element of the potential from the cell centred at $\vec{R}_\ell$ is

$$\int^1 \psi_{k+G}(\vec{r})V(\vec{r})\psi_k(\vec{r})d\vec{r}$$

$$= \int^1 e^{-i(\vec{k}+\vec{G})\cdot\vec{r}}\, u_{k+G}(\vec{r})V(\vec{r})e^{i\vec{k}\cdot\vec{r}}\, u_k(\vec{r})d\vec{r}$$

By changing the variable of integration, this equals

$$\int e^{-i(\vec{k}+\vec{G})\cdot(\vec{r}+\vec{R}_\ell)}\, u_{k+G}(\vec{r}+\vec{R}_\ell)V(\vec{r}+\vec{R}_\ell)e^{i\vec{k}\cdot(\vec{r}+\vec{R}_\ell)}\, x$$

$$u_k(\vec{r}+\vec{R}_\ell)d(\vec{r}+\vec{R}_\ell)$$

Using the periodicity of $u_k(\vec{r})$ and $V(\vec{r})$ and noting that

$e^{i\vec{G}\cdot\vec{R}_\ell} = 1$, this equals

$$\int e^{-i(\vec{k}+\vec{G})\cdot\vec{r}}\, u_{k+G}(\vec{r})V(\vec{r})\, e^{i\vec{k}\cdot\vec{r}}\, u_k(\vec{r})d\vec{r}$$

which is the same as the contribution from the cell at $\vec{r}=o$. The same result holds for the matrix elements of ∇^2 and unity. Hence in evaluating these matrix elements it is sufficient to limit the range of integration to the cell at the origin of direct space only, assuming the functions to be of the Bloch form and remembering that conditions (1-5) apply.

Let $|\psi_c\rangle \equiv |\psi_{n\ell m}\rangle$ denote the orthonormal set of core state solutions of (1-1) for a specific wave vector. The following discussion will deal with this single wave vector only. Define a projection operator, P, by

$$P = 1 - \sum_c |\psi_c\rangle\langle\psi_c|$$

Acting on an arbitrary function this operator deletes that part of the function which is in the Hilbert space of the core states. An orthogonalized plane wave is defined by

$$|\phi(k)\rangle = P|k\rangle = |k\rangle - \sum_c \langle\psi_c|k\rangle|\psi_c\rangle \qquad (1\text{-}6)$$

where $|k\rangle$ denotes a plane wave of wave vector $\vec{k}$. Since the plane waves constitute a complete set, the OPW's are sufficient to represent any function in the Hilbert subspace of the conduction states. The $\langle\psi_c|k\rangle$'s are the orthogonality coefficients specifying the amount of each core function which must be subtracted from the plane wave to attain orthogonality.

Express the conduction solution $|\psi\rangle$ in terms of OPW's:

$$|\psi\rangle = \sum_k a_k |\phi(k)\rangle$$

Then, by the variational principle, the expectation value of the Hamiltonian will reach its minimum value W, with the set of coefficients a_k, when the following matrix equation is satisfied:

$$\left[[H] - W[s]\right]\left[a\right] = o \qquad (1\text{-}7a)$$

where square brackets denote matrices,

$$H_{ij} = \langle\phi(k_i)|H|\phi(k_j)\rangle$$
$$S_{ij} = \langle\phi(k_i)|\phi(k_j)\rangle$$

and $[a]$ is the column matrix with elements a_k. W is a solution when the determinant of the coefficients vanishes:

$$\left|[H] - W[s]\right| = o \qquad (1\text{-}7b)$$

Evaluation of Matrix Elements

The matrix elements H_{ij} and S_{ij} are now evaluated:

$$\begin{aligned} H_{ij} &= \langle\phi(k_i)|H|\phi(k_j)\rangle \\ &= \langle k_i|PHP|k_j\rangle \\ &= \langle k_i|(1-\sum_{c'}|\psi_{c'}\rangle\langle\psi_{c'}|)H(1-\sum_{c}|\psi_{c}\rangle\langle\psi_{c}|)|k_j\rangle \\ &= \langle k_i|H|k_j\rangle - \sum_{c'}\langle k_i|\psi_{c'}\rangle\langle\psi_{c'}|H|k_j\rangle - \sum_{c}\langle k_i|H|\psi_{c}\rangle\langle\psi_{c}|k_j\rangle \\ &\quad + \sum_{c'}\sum_{c}\langle k_i|\psi_{c'}\rangle\langle\psi_{c'}|H|\psi_{c}\rangle\langle\psi_{c}|k_j\rangle \end{aligned}$$

Using $H|\psi_c\rangle = E_c|\psi_c\rangle$ and $\langle\psi_{c'}|\psi_c\rangle = \delta_{c'c}$,

$$H_{ij} = \langle k_i|H|k_j\rangle - \sum_{c'} E_{c'}\langle k_i|\psi_{c'}\rangle\langle\psi_{c'}|k_j\rangle$$

$$- \sum_c E_c\langle k_i|\psi_c\rangle\langle\psi_c|k_j\rangle + \sum_c E_c\langle k_i|\psi_c\rangle\langle\psi_c|k_j\rangle$$

$$H_{ij} = \langle k_i|H|k_j\rangle - \sum_c E_c\langle k_i|\psi_c\rangle\langle\psi_c|k_j\rangle \qquad (1\text{-}8a)$$

Similarly,

$$S_{ij} = \langle\phi(k_i)|\phi(k_j)\rangle$$

$$= \langle k_i|k_j\rangle - \sum_c\langle k_i|\psi_c\rangle\langle\psi_c|k_j\rangle \qquad (1\text{-}8b)$$

The plane waves and core functions are chosen to have normalization unity in a unit cell of volume Ω_o. The plane wavesin the r representation are then:

$$\langle r|k\rangle = \frac{1}{\sqrt{\Omega_o}}\ e^{i\vec{k}\cdot\vec{r}}.$$

The OPW method as described is only useful if the core functions are easily determined. This will be the case if the potential is spherical about a lattice site within a sphere of some radius r_o and the atomic-like core solutions of this spherical potential vanish at $r<r_o$. The core solutions in the cell are then readily calculated by the methods of atomic physics and are of the form:

$$\langle r|\psi_c\rangle = \frac{P_{n\ell}(r)}{r}\ Y_{\ell m}(\theta,\phi) \qquad (1\text{-}9)$$

It will be assumed below that the core electrons fill closed shells.

The matrix elements of (1-8) will now be evaluated. Recall that the integration is only over the unit cell at the origin of direct space and, by (1-5), the matrix elements vanish unless they connect states with wave vectors differing by a reciprocal lattice vector.

$$\langle k_i | k_j \rangle = \frac{1}{\Omega_o} \int e^{-i\vec{k}_i \cdot \vec{r}} \, e^{i\vec{k}_j \cdot \vec{r}} \, d\vec{r}$$

$$= \delta_{\vec{k}_i \vec{k}_j}$$

$$\langle k_i | H | k_j \rangle = \frac{1}{\Omega_o} \int e^{-i\vec{k}_i \cdot \vec{r}} \, (-\nabla^2 + V(\vec{r})) e^{i\vec{k}_j \cdot \vec{r}} \, d\vec{r}$$

$$= k_j^2 \delta_{\vec{k}_i \vec{k}_j} + v(\vec{G_{ij}})$$

where

$$v(\vec{G}) \equiv \frac{1}{\Omega_o} \int e^{-i\vec{G} \cdot \vec{r}} \, V(\vec{r}) d\vec{r} \qquad (1\text{-}10)$$

and G_{ij} is the reciprocal lattice vector joining $\vec{k_i}$ to $\vec{k_j}$.

$$\langle \psi_c | k \rangle = \frac{1}{\sqrt{\Omega_o}} \int \frac{P_{n\ell}(r)}{r} \, Y^*_{\ell m}(\theta, \phi) e^{i\vec{k} \cdot \vec{r}} \, d\vec{r}$$

Expanding the plane wave in spherical harmonics,

$$\langle \psi_c | k \rangle = \frac{4\pi}{\sqrt{\Omega_o}} \int \sum_{\ell'=o}^{\infty} \sum_{m'=-\ell'}^{\ell'} i^{\ell'} j_{\ell'}(kr) Y^*_{\ell' m'}(\theta_k, \phi_k) Y_{\ell' m'}(\theta_r, \phi_r) x$$

$$\frac{P_{n\ell}(r)}{r} \, Y^*_{\ell m}(\theta, \phi) \, r^2 dr d\alpha$$

where $d\alpha \equiv \sin\theta d\theta d\phi$ and $\theta_k, \phi_k, \theta_r$ and ϕ_r denote the direction of the $\vec{k}$ and $\vec{r}$ vectors. Therefore,

$$\langle \psi_c | k \rangle = F_{n\ell}(k)\ Y^*_{\ell m}\ (\theta_k, \phi_k)$$

where

$$F_{n\ell}(k) = \frac{4\pi}{\sqrt{\Omega_o}}\ i^{\ell} \int_o^{\infty} \frac{P_{n\ell}(r)}{r}\ j_{\ell}\ (kr) r^2 dr \qquad (1\text{-}11)$$

Hence, the second term in (1-8a) becomes

$$\sum_{n\ell m} E_{n\ell}\ \langle k_i | \psi_{n\ell m} \rangle \langle \psi_{n\ell m} | k_j \rangle$$

$$= \sum_{n\ell} E_{n\ell}\ F^*_{n\ell}(k_i)\ F_{n\ell}(k_j) \sum_{m=-\ell}^{\ell} Y_{\ell m}(\theta_{k_i}, \phi_{k_i}) Y^*_{\ell m}(\theta_{k_j}, \phi_{k_j})$$

Using the addition theorm for spherical harmonics, this equals

$$\frac{1}{4\pi} \sum_{n\ell} (2\ell+1) E_{n\ell} F^*_{n\ell}(k_i)\ F_{n\ell}\ (k_j)\ P_{\ell}(\cos\theta_{ij})$$

where θ_{ij} denotes the angle between $\vec{k_i}$ and $\vec{k_j}$ and $P_{\ell}(x)$ is the Legendre polynomial. The OPW matrix elements are, then, for the case of a Bravais lattice:

$$H_{ij} = k_j^2\ \delta_{\vec{k_i}\vec{k_j}} - \frac{1}{4\pi} \sum_{n\ell} (2\ell+1) E_{n\ell} F^*_{n\ell}(k_i) F_{n\ell}(k_j) P_{\ell}(\cos\theta_{ij}) \qquad (1\text{-}12a)$$

$$S_{ij} = \delta_{\vec{k_i}\vec{k_j}} - \frac{1}{4\pi} \sum_{n\ell} (2\ell+1) F^*_{n\ell}(k_i) F_{n\ell}(k_j) P_{\ell}(\cos\theta_{ij}) \qquad (1\text{-}12b)$$

Pseudopotential Theory*

Phillips and Kleinman (PK59) showed that the OPW

---

*Only the Phillips and Kleinman formulation of the pseudopotential and its relation to the OPW method are discussed here. For a discussion of more recent work see the book by Harrison (Ha66).

method is equivalent to a plane wave variational solution of Schrödinger's equation with the potential replaced by a pseudopotential. Expanding the solution in OPW's (an infinite number if necessary),

$$|\psi\rangle = \sum_k a_k |\phi(k)\rangle .$$

Substituting in Schrödinger's equation,

$$\sum_k a_k H|\phi(k)\rangle = E \sum_k a_k |\phi(k)\rangle$$

$$\sum_k a_k H(1- \sum_c |\psi_c\rangle\langle\psi_c|)k\rangle = E \sum_k a_k (1-\sum_c |\psi_c\rangle\langle\psi_c|)k\rangle$$

Using $H|\psi_c\rangle = E_c|\psi_c\rangle$ and collecting terms,

$$\sum_k a_k (H+ \sum_c (E-E_c)|\psi_c\rangle\langle\psi_c|)k\rangle = E \sum_k a_k |k\rangle$$

which is equivalent to assuming a plane wave trial solution $\sum_k a_k|k\rangle$ to solve the equation with an effective Hamiltonian

$$- \nabla^2 + V(\vec{r}) + V_R,$$

where $V_R \equiv \sum_c (E-E_c)|\psi_c\rangle\langle\psi_c|$

is an effective repulsive potential. The pseudopotential is $V + V_R$. Since V is attractive, cancellation will occur. If the cancellation is such that the pseudopotential nearly vanishes then the single plane wave $|k\rangle$ is a good approximation to the solution in the pseudopotential formulation; this corresponds to a one-OPW solution. Note that the pseudopoten-

tial is state dependent through E.

Phillips and Kleinman have compared the Fourier transforms of the attractive and effective repulsive potentials in silicon for the cases of an s-like state and a p-like state, as shown in Figs. 1. In the s case the cancellation is seen to be good at large k; however, the same is not true in the p case. They state that the orthogonalization procedure can be regarded as a way of including the radial kinetic energy in the core region, but not the angular kinetic energy. (In the p case, if the angular kinetic energy $\ell(\ell+1)/r^2$ is explicitly added to the repulsive potential, then the cancellation (Fig. 1(b)) is seen to be as full as in the s case.) Then, orthogonalization to the core states makes an OPW trial function a good approximation in the case of an s-state, a poorer approximation for a p-state and a very poor one in the d-band case.

There is a second problem hindering the application of the OPW method to d-bands. The outer "core" functions, such as the 4s and 4p in niobium*, do not vanish at a radius less than half the nearest neighbor distance, but typically have values of $P_{4s} \cong 0.1_{\infty}$ and $P_{4p} \cong 0.2$ for atomic-like wave functions normalized to $\int_0 P_{n\ell}^2 \, dr=1$. These states are, then, not completely localized but rather form very narrow bands. This prevents proper orthogonalization of the plane waves to

---

*The outer atomic configuration of niobium is $(4s)^2(4p)^6(4d)^4(5s)^1$.

these states by the usual techniques; the numerical error introduced by improper orthogonalization becomes important when a large number of OPW's are included in the secular equation. If no attempt is made to orthogonalize to these states the lowest roots of the secular equation will correspond to these levels and the next highest solutions will correspond to the conduction band states. Such a procedure is unsatisfactory for two reasons: First, OPW's are plane wave-like in the interstitial regions and so are not well suited to represent the exponential behavior of core levels; secondly, it is a well known fact (MM43) that a small deviation from full convergence in the lowest root of a secular equation can lead to considerably larger deviations from the correct solution in higher roots.

Crystalline Potential

No mention has yet been made of the explicit form of the crystalline potential. It is often most convenient to approximate it as a sum of spherical potentials centred on lattice sites,

$$V(\vec{r}) = \sum_{\ell} V_{at}(|\vec{r}-\vec{R}_{\ell}|) \qquad (1\text{-}13)$$

where $V_{at}(r)$ is a spherical atomic-like potential. In the present work $V_{at}(r)$ is constructed by overlapping free atom charge densities (see Chapter 3 for a more detailed discussion). Sometimes the conduction electrons have been approximated by plane waves and their contribution converted into a suitable spherical average about each lattice site.

However, this sometimes raises the problem of correcting for the overlap (e.g. for the case in which the conduction electrons are represented by a uniform charge distribution in the Wigner-Seitz sphere). Sometimes V is approximated by a sum of non-overlapping potentials, as in the muffin-tin form of V_{at} used to date in APW calculations. Overlap is advantageous from the point of view of building more of the correct directional asymmetry into the crystalline potential inside a particular unit cell.

The potential explicitly enters an OPW calculation in two ways: first, it is required in direct space to solve for the core states; secondly, its Fourier transforms, $v(\vec{G})$, are required in the OPW matrix elements. Golin (G65) has divided the total potential into two contributions, core and valence. The core contribution is expressed in the form (1-13); the valence contribution is handled principally by its Fourier transforms. This is a particularly convenient formulation for self-consistent calculations. The core potential is not varied throughout the calculation. After the first trial the Fourier transforms of the valence potential are directly determined from the band structure; this valence potential is then transformed into real space, spherically averaging about a lattice site, to allow calculation of the core states.

Using (1-13) and expanding $e^{i\vec{G}\cdot\vec{r}}$ in spherical harmonics, (1-10) takes the form (with or without overlap):

$\vec{G} \neq o$:

$$v(\vec{G}) = \frac{4\pi}{G\Omega_o} \int_o^\infty rV_{at}(r)\sin(\vec{G}\cdot\vec{r})\,dr \qquad (1\text{-}14a)$$

$\vec{G} = o$:

$$v(o) = \frac{4\pi}{\Omega_o} \int_o^\infty r^2 V_{at}(r)\,dr \qquad (1\text{-}14b)$$

Symmetrized Combinations

As discussed above, the trial functions to be used in the OPW band structure calculation at point $\vec{k}$ in the first Brillouin zone are the OPW's of wave vector $\overrightarrow{k + G}$ for many reciprocal lattice vectors $\vec{G}$. In practice, however, the order of the secular equation can be greatly reduced at symmetry points of the zone: If the trial functions are taken to be linear combinations of OPW's which transform under rotation according to the columns of the irreducible representations of the group of the wave vector $\vec{k}$, then, by theorems of group theory, e.g. (Ti64), matrix elements of the Hamiltonian and of unity will vanish between functions which do not correspond to the same column of the same irreducible representation. Hence the secular determinant is effectively reduced to a number of lower order determinantal blocks along the diagonal, each of which can then be solved distinctly. The symmetrized combinations for many structures can be determined, for example, from Schlosser's generators (S62),and have also been tabulated by Luehrmann (L66).

APW Method

Consider first the augmented plane wave method applied to a muffin-tin potential, that is, a potential of the form (1-13) for which the spherical potential contributions on neighboring lattice sites do not mutually overlap. The idea of the APW method is to solve for each band wave function exactly in the muffin-tin sphere about each lattice point and variationally by plane waves in the interstitial regions. At each point $\vec{k}$ in the first zone consider choosing a trial energy value E, representing an estimate of the energy at that point in the particular band under consideration. For that energy the solution within the sphere is of the form:

$$\sum_{\ell,m} a_{\ell m} Y_{\ell m}(\theta,\phi)\, R_{\ell}(E,r)$$

where the radial wave functions have been integrated outwards from r=o for that energy and all values of ℓ and m are to be included in the summation. The coefficients $a_{\ell m}$ are chosen so that this interior solution will match continuously to a plane wave at the sphere surface. The APW is then:

$$\phi(k) = a_o \varepsilon(r-r_i) e^{i\vec{k}\cdot\vec{r}} + \sum_{\ell,m} a_{\ell m}\, \varepsilon(r_i-r)\, Y_{\ell m}(\theta,\phi)\, R_{\ell}(E,r) \qquad (1\text{-}15)$$

where ε is a unit step function:

$$\varepsilon(x) = 1 \text{ for } x \geq o$$

$$\varepsilon(x) = o \text{ for } x < o$$

and r_i is the radius of the muffin-tin sphere. Consider expanding the plane wave in spherical harmonics about the lattice point; then each radial component, proportional to $j_\ell(kr)$, must be matched to the interior radial solution, $R_\ell(E,r)$, so that the coefficients are:

$$a_{\ell m} = 4\pi i^\ell a_o Y^*_{\ell m}(\theta_k,\phi_k) \frac{j_\ell(k\ r_i)}{R_\ell(E,r_i)}$$

Note that the slope of each spherical harmonic component is discontinuous, in general, at $r=r_i$; only the amplitudes have been matched.

The set of APW's with wave vectors = $\vec{k}+\vec{G_i}$ is formed for a certain number of reciprocal lattice vectors $\vec{G_i}$ and the trial solution is expanded in terms of these APW's. (In practice, symmetrized combinations of APW's are used at symmetry points; also, values of ℓ greater than about 12 are ignored.) The desired solution E must satisfy a secular determinant:

$$| [H] - E [S] | = o \qquad (1\text{-}16)$$

where the notation is as in equations (1-7). Note that $[H]$ and $[S]$ are dependent on E because of the form of the solution in the interior of the sphere and also through the matching coefficients $a_{\ell m}$. The determinant (1-16) is computed as a function of E (involving radial integrations for each value of E) and the zeros of the function are found. This procedure is repeated as more reciprocal lattice vectors

$\vec{G}_i$ are included and continues until the solution is considered to be converged. This is done separately for each value of $\vec{k}$ and for each band of interest.

The problems which arise in applying the OPW method to d-bands do not occur in the APW approach. First, the orthogonalization to the outer core levels is not a problem since the core levels need not be computed; secondly, the inappropriateness of plane wave components to represent d-bands is lessened because in practice the muffin-tin sphere is usually chosen to have a radius of half the nearest-neighbor distance and so the interstitial region to be represented by plane waves is quite small.

No application of the APW method has yet been made for a potential other than a muffin-tin. Slater has proposed a perturbation approach for such a case (Sl65). It also seems clear that in many cases the problem can be solved exactly by considering the analogy between APW's and OPW's (Sl65).

CHAPTER 2

MODIFIED OPW METHOD

As mentioned previously, difficulties arise in applying the OPW method to transition metals. Such an application would be useful, however, since the OPW method is formally simpler than the APW and has also been the basis of the self-consistent band structure methods developed so far; in addition, several applications of band structures have made use of one-OPW and pseudopotential approximations for simple metals and it would be useful if such work could be extended to transition metals.

To the knowledge of the author the only successful application of the OPW method in the transition region is that of Callaway (C55a, C55b) to the energy bands of iron. In that case the s-bands were treated by the cellular method while the p- and d-bands were expanded in OPW's. To obtain convergence for the d-band points it was found necessary to add to the set of OPW's a function which is atomic d-like near the lattice site and vanishes in the interstitial regions. The addition of such cut-off functions is the basis of the modified OPW method employed in the present calculation, so Callaway's work will now be described in a little more detail.

In iron the occupied conduction bands arise principally from the 3d and 4s atomic levels. For those d-like points in the Brillouin zone which contain no s or p character (e.g. $\Gamma_{25'}$) the appropriate symmetrized combinations of OPW's contain spherical harmonic components of $\ell \geq 2$ only. Since there are no core states with $\ell \geq 2$, no orthogonalization terms appear in these symmetrized combinations; thus the OPW expansion is identical to a plane wave expansion for these states. Callaway found the convergence to be very poor in such cases because it takes an exceedingly large number of plane waves to represent the rapid variation of the d-band wave functions near the core. This problem was overcome by adding to the basis set a function which represents the behavior well near the nucleus and which vanishes with vanishing derivatives at the Wigner-Seitz cell boundary; this very much improved the d-band convergence in the iron calculations.

The atomic configuration of niobium is $(1s)^2(2s)^2(2p)^6(3s)^2(3p)^6(3d)^{10}(4s)^2(4p)^6(4d)^4(5s)^1$. The occupied conduction bands arise principally from the 4d and 5s levels. The 4s and 4p states are the troublesome core levels: the atomic functions on adjacent lattice sites overlap slightly but enough to prevent proper orthogonalization of the plane waves to these states. A difference from the case of iron is that d-like symmetrized combinations of OPW's contain

terms representing orthogonalization to the 3d level; however, as discussed in the preceding chapter, this does not provide much help because the OPW method does not work well for d-like states. As in Callaway's case this problem was overcome by adding to the set of OPW's a function which is similar to the 4d atomic state near the lattice site but which vanishes before half the nearest neighbor distance. It is necessary to orthogonalize this cut-off function to the 3d core level since the variational principle is to be used. The problem of the troublesome 4s and 4p core levels was overcome in a similar way: Cut-off functions similar to 4s and 4p atomic states, but orthogonal to the lower states, were also added to the basis set, while the plane waves were orthogonalized to the levels up to and including the 3d only. For an s-like point, then, the lowest root of the secular equation corresponds to the 4s core level and the next lowest root is the desired s-like conduction band level. This was found to be a successful way of handling the outer core states. Since the atomic-like 4s and 4p solutions of the crystalline potential have small amplitudes at the cell boundary they need only be modified slightly to be converted into cut-off functions. The variational calculation then quickly converges to these levels; since the solutions of the secular equation corresponding to different roots are mutually orthogonal, the proper orthogonalization

is thereby introduced into the conduction band solutions.

In summary, then, the basis set consists of 4s-, 4p- and 4d-like cut-off functions and plane waves which have been orthogonalized to the core levels up to and including the 3d only. The formulation of the cut-off functions and the derivation of the additional matrix elements required by the introduction of the cut-off functions are now given.

Lattice Harmonics and the Cut-Off Functions

Define a cut-off function

$$\phi^{CO}_{n\ell m}(\vec{r}) = \frac{P^{CO}_{n\ell}(r)}{r} Y_{\ell m}(\theta,\phi) \qquad (2\text{-}1)$$

$P^{CO}_{n\ell}$ is to be similar to the atomic-like solution near the lattice site; $\phi^{CO}_{n\ell m}$ must be orthogonal to the lower core states and $P^{CO}_{n\ell}$ must vanish at some radius less than half the nearest neighbor distance. Also define

$$H\phi^{CO}_{n\ell m}(\vec{r}) \equiv E^{CO}_{n\ell} \frac{G^{CO}_{n\ell}(r)}{r} Y_{\ell m}(\theta,\phi) \qquad (2\text{-}2)$$

This defines only the product $E^{CO}_{n\ell} G^{CO}_{n\ell}$. For the present this is sufficient; its usefulness will be clarified later.

In principle it is necessary to include in the basis set all values of m corresponding to each nℓ value. In practice, however, the problem is simplified: Symmetrized combinations of spherical harmonics of different m values can be formed which transform according to the columns of the

irreducible representations of the group of the wave vector. By group theory the matrix elements of the Hamiltonian and of unity vanish between combinations unless they belong to the same column of the same irreducible representation. These linear combinations are called lattice harmonics. For example, in solving for the level Γ_{25}, it is necessary to include only the combination $\frac{1}{i\sqrt{2}}(Y_{21}+Y_{2-1})$ with symmetrized combinations of OPW's chosen to transform as yz. The lattice harmonics have been tabulated at all the symmetry points of several structures by Bell (B54).

Since the lattice harmonics are real it is convenient to derive the cut-off matrix elements in terms of real angular wave functions which are here defined by:

For m≠o:

$$y_{\ell mj}(\theta,\phi) \equiv \frac{(-i)^j}{i^m\sqrt{2}}\left(Y_{\ell m}(\theta,\phi) + (-1)^j Y_{\ell -m}(\theta,\phi)\right) \qquad (2\text{-}3)$$

where j takes on the values o and 1 only.

For m=o:

$$y_{\ell oo}(\theta,\phi) \equiv Y_{\ell o}(\theta,\phi)$$

The real angular wave functions are listed in Table 1. The lattice harmonic combinations of these real angular wave functions are given in Table 2.

As an example,

$$y_{110} = \frac{1}{i\sqrt{2}}(Y_{11}+Y_{1-1}) = -\sqrt{\frac{3}{4\pi}}\sin\theta\sin\phi = -\sqrt{\frac{3}{4\pi}}\frac{y}{r}$$

$$y_{111} = -\frac{1}{\sqrt{2}}(Y_{11}-Y_{1-1}) = \sqrt{\frac{3}{4\pi}}\sin\theta\cos\phi = \sqrt{\frac{3}{4\pi}}\frac{x}{r}$$

$$y_{100} = Y_{10} = \sqrt{\frac{3}{4\pi}}\cos\theta = \sqrt{\frac{3}{4\pi}}\frac{z}{r}$$

It is convenient that the matrix elements of the cut-off functions with the OPW's be real. To this end the normalization of the cut-off functions is chosen in the following way:

$$\phi^{co}_{n\ell mj} = (i)^{-\ell} \frac{P^{co}_{n\ell}(r)}{r} Y_{\ell mj} \qquad (2\text{-}4)$$

Using (2-1) and (2-3),

$$\phi^{co}_{n\ell mj} = \frac{(i)^{-\ell}(-i)^{j}}{i^{m}\sqrt{2}} (\phi^{co}_{n\ell m} + (-1)^{j}\phi^{co}_{n\ell -m}) \qquad (2\text{-}5)$$

The desired matrix elements are then:

$$\langle \phi^{co}_{n'\ell'm'j'} | H | \phi^{co}_{n\ell mj} \rangle$$

$$\langle \phi^{co}_{n'\ell'm'j'} | \phi^{co}_{n\ell mj} \rangle$$

$$\langle \phi^{co}_{n\ell mj} | H | \phi(k) \rangle$$

$$\langle \phi^{co}_{n\ell mj} | \phi(k) \rangle$$

where $\phi(k)$ is an orthogonalized plane wave given in the unit cell by

$$\phi(k) = \frac{1}{\sqrt{\Omega_o}} e^{i\vec{k}\cdot\vec{r}} - \sum_{\substack{n\ell m \\ (core)}} B_{n\ell}(k)\psi_{n\ell m}(\vec{r}) \qquad (2\text{-}6)$$

where $B_{n\ell}(k) \equiv \frac{1}{\sqrt{4\pi(2\ell+1)}} F_{n\ell}(k)$

and $F_{n\ell}(k)$ is defined by (1-11).

Matrix Elements

Consider first the case $m \neq o$. It is convenient to evaluate

$$\langle \phi^{CO}_{n'\ell'm'} | H | \phi^{CO}_{n\ell m} \rangle$$

$$= \int \frac{P^{CO}_{n'\ell'}}{r} \; Y^{*}_{\ell'm'}(\theta,\phi) \; E^{CO}_{n\ell} \; \frac{G^{CO}_{n\ell}(r)}{r} \; Y_{\ell m}(\theta,\phi) r^2 dr d\alpha$$

(where $d\alpha \equiv \sin\theta d\theta d\phi$)

$$= E^{CO}_{n\ell} \; \delta_{\ell\ell'} \; \delta_{mm'} \; I(P^{CO}_{n'\ell'}, G^{CO}_{n\ell}) \qquad (2\text{-}7)$$

where $$I(P^{CO}_{n'\ell'}, G^{CO}_{n\ell}) \equiv \int_o^\infty P^{CO}_{n'\ell'}(r) \; G^{CO}_{n\ell}(r) dr \qquad (2\text{-}8)$$

Similarly,

$$\langle \phi^{CO}_{n'\ell'm'} | \phi^{CO}_{n\ell m} \rangle = \delta_{\ell\ell'} \; \delta_{mm'} \; I(P^{CO}_{n'\ell'}, P^{CO}_{n\ell}) \qquad (2\text{-}9)$$

Using (2-5), (2-7) and (2-9),

$$\langle \phi^{CO}_{n'\ell'm'j'} | H | \phi^{CO}_{n\ell mj} \rangle = \delta_{\ell\ell'} \; \delta_{mm'} \; \delta_{jj'} \; E^{CO}_{n\ell} I(P^{CO}_{n'\ell'}, G^{CO}_{n\ell}) \qquad (2\text{-}10a)$$

and

$$\langle \phi^{CO}_{n'\ell'm'j'} | \phi^{CO}_{n\ell mj} \rangle = \delta_{\ell\ell'} \; \delta_{mm'} \; \delta_{jj'} \; I(P^{CO}_{n'\ell'}, P^{CO}_{n\ell}) \qquad (2\text{-}10b)$$

It is easily seen that equations (2-10) hold also for the case m=o.

In order to evaluate the matrix elements of the Hamiltonian between the cut-off functions and the OPW's first consider

$$\langle \phi^{CO}_{n\ell m} | H | \phi(k) \rangle$$

$$= \langle \phi^{CO}_{n\ell m} | H | k \rangle - \sum_{\substack{n'\ell'm' \\ (core)}} B_{n'\ell'}(k) \langle \phi^{CO}_{n\ell m} | H | \psi_{n'\ell'm'} \rangle$$

But, $\langle \phi^{CO}_{n\ell m} | H | \psi_{n'\ell'm'} \rangle = E_{n'\ell'} \langle \phi^{CO}_{n\ell m} | \psi_{n'\ell'm'} \rangle = 0$

because the cut-off functions have been explicitly orthogonalized to the core functions. Hence,

$$\langle \phi^{CO}_{n\ell m} | H | \phi(k) \rangle = \langle \phi^{CO}_{n\ell m} | H | k \rangle$$

$$= E^{CO}_{n\ell} \int \frac{G^{CO}_{n\ell}(r)}{r} Y^*_{\ell m}(\theta,\phi) \frac{1}{\sqrt{\Omega_o}} e^{i\vec{k}\cdot\vec{r}} r^2 dr d\alpha$$

Expanding the plane wave in spherical harmonics this reduces to

$$\frac{4\pi E^{CO}_{n\ell}}{\sqrt{\Omega_o}} i^{\ell} Y^*_{\ell m}(\theta_k,\phi_k) I\left(G^{CO}_{n\ell}, rj_{\ell}(k)\right) \qquad (2\text{-}11)$$

where $I\left(G^{CO}_{n\ell}, rj_{\ell}(k)\right) \equiv \int_o^{\infty} G^{CO}_{n\ell}(r)\, rj_{\ell}(kr)\, dr$

Using (2-5), (2-1), (2-3) and (2-11) it follows that for $m \neq o$

$$\langle \phi^{CO}_{n\ell mj} | H | \phi(k) \rangle = (-)^{\ell} \frac{4\pi}{\sqrt{\Omega_o}} E^{CO}_{n\ell} y_{\ell mj}(\theta_k,\phi_k) I\left(G^{CO}_{n\ell}, rj_{\ell}(k)\right) \qquad (2\text{-}12a)$$

Similarly,

$$\langle \phi^{co}_{n\ell mj} | \phi(k) \rangle = (-)^{\ell} \frac{4\pi}{\sqrt{\Omega_o}} Y_{\ell mj}(\theta_k, \phi_k) \; I \left\langle P^{co}_{n\ell}, rj_{\ell}(k) \right\rangle \quad (2\text{-}12b)$$

It is easily seen that equations (2-12) hold also for the case m=o.

Form of Cut-Off Functions

The explicit form of the cut-off radial wave function, $P^{co}_{n\ell}(r)$, has not as yet been mentioned. The procedure is to integrate the radial Schrödinger equation outwards from r=o for the correct ℓ-value for some appropriate energy $E^{co}_{n\ell}$. This function is then cut off at some $r=r_m$ and a tail is joined smoothly to it; the tail is chosen to vanish at some $r=r_{\ell}$ which is less than or equal to half the nearest neighbor distance. Let the product of r and the radial wave function for this $E^{co}_{n\ell}$ be denoted by $Q^{co}_{n\ell}(r)$. In this work the tail has been chosen so that the unorthogonalized cut-off radial wave function, denoted by $S^{co}_{n\ell}(r)$, is given by:

$$S^{co}_{n\ell}(r) = \begin{cases} Q^{co}_{n\ell}(r) \text{ for } o<r<r_m & (2\text{-}13a) \\ a\left(1 + \cos q(r-r_o)\right) \text{ for } r_m<r<r_{\ell} & (2\text{-}13b) \end{cases}$$

The three parameters a, q and r_o are chosen to satisfy the three conditions that the tail match $Q^{co}_{n\ell}$ continuously with continuous first derivative at $r=r_m$ and vanish identically

at $r=r_\ell$. Specifically,

$$a = \frac{Q^{co}_{n\ell}(r_m)}{1 + \cos q\,(r_m - r_o)} \tag{2-14}$$

$$q = \frac{\pi}{r_\ell - r_o} \tag{2-15}$$

and r_o is determined by a trial and error procedure: For each trial value of r_o, q is determined by (2-15) and then a is found by (2-14). The slopes of (2-13a) and (2-13b) are compared at $r=r_m$ and the trial and error procedure continues until the slope of (2-13b) equals that of (2-13a).

$S^{co}_{n\ell}(r)$ must then be orthogonalized to the core functions of the same angular momentum ℓ, so the final (orthogonalized) cut-off function is

$$P^{co}_{n\ell}(r) = S^{co}_{n\ell}(r) - \sum_{n'} a^{co}_{n'\ell} P_{n'\ell}(r) \tag{2-16}$$

where $a^{co}_{n'\ell} = \int_0^\infty P_{n'\ell}(r)\, S^{co}_{n\ell}(r)\, dr$

and $\sum_{n'}$ is a sum over core states of angular momentum ℓ.

The application of the Hamiltonian to the cut-off function is now shown.

$$H\phi^{co}_{n\ell m}(r) = H \frac{P^{co}_{n\ell}(r)}{r} Y_{\ell m}(\theta,\phi)$$

For $o \leq r \leq r_m$:

From (2-16) and (2-13a),

$$H\phi^{co}_{n\ell m}(r) = H\left(\frac{Q^{co}_{n\ell}(r)}{r} - \sum_{n'} a^{co}_{n'\ell}\frac{P_{n'\ell}(r)}{r}\right) Y_{\ell m}(\theta,\phi)$$

$$= \left(E^{co}_{n\ell}(r)\frac{Q^{co}_{n\ell}(r)}{r} - \sum_{n'} E_{n'\ell}\, a^{co}_{n'\ell}\frac{P_{n'\ell}(r)}{r}\right) Y_{\ell m}(\theta,\phi)$$

Then, from (2-2),

$$G^{co}_{n\ell}(r) = Q^{co}_{n\ell}(r) - \frac{1}{E^{co}_{n\ell}} \sum_{n'} E_{n'\ell}\, a^{co}_{n'\ell}\, P_{n'\ell}(r) \qquad (2\text{-}17a)$$

For $r_m \leq r \leq r_\ell$:

From (2-16) and (2-13b),

$$H\phi^{co}_{n\ell m}(r) = A + B$$

where

$$A = H\left(\frac{a(1+\cos q(r-r_o))}{r} Y_{\ell m}(\theta,\phi)\right)$$

and

$$B = H\left(-\sum_{n'} a^{co}_{n'\ell}\frac{P_{n'\ell}(r)}{r} Y_{\ell m}(\theta,\phi)\right)$$

Immediately,

$$B = -\sum_{n'} E_{n'\ell}\, a^{co}_{n'\ell}\frac{P_{n'\ell}(r)}{r} Y_{\ell m}(\theta,\phi)$$

$$A = \left(-\nabla^2 + V_{at}(r)\right)\left(\frac{a(1+\cos q(r-r_o))}{r} Y_{\ell m}(\theta,\phi)\right)$$

$$= \frac{Y_{\ell m}(\theta,\phi)}{r}\left(-\frac{d^2}{dr^2} + \frac{\ell(\ell+1)}{r^2} + V_{at}(r)\right)\left(a(1+\cos q(r-r_o))\right)$$

$$= \frac{Y_{\ell m}(\theta,\phi)}{r}\left\{aq^2\cos q(r-r_o) + a(1+\cos q(r-r_o))\times \left(\frac{\ell(\ell+1)}{r^2} + V_{at}(r)\right)\right\}$$

So,

$$G^{co}_{n\ell}(r) = \frac{1}{E^{co}_{n\ell}(r)} \left\{ aq^2 \cos q(r-r_o) + a(1+\cos q(r-r_o)) \left(\frac{\ell(\ell+1)}{r^2} + V_{at}(r) \right) - \sum_{n'} E_{n'\ell}\, a^{co}_{n'\ell}\, P_{n'\ell}(r) \right\} \quad (2\text{-}17b)$$

It should be noted that only the first derivative of the tail of the cut-off function has been matched at $r=r_m$. This means that, in general, the second derivative is discontinuous at r_m as well as at r_ℓ. (At the latter point the tail is a cosine function at its extremum and therefore has a non-vanishing second derivative.) These discontinuities must be kept in mind when applying the kinetic energy operator to the cut-off function. Specifically, $G^{co}_{n\ell}$ is discontinuous at these points and so the integrals involving $G^{co}_{n\ell}$ must be evaluated accordingly.

It should also be noted that there is no restriction to a muffin-tin potential in this modified OPW method. However, if the potential is of the form (1-13) with overlapping spherical contributions then the cut-off functions must be made to vanish at a radius such that they do not extend into the overlap region; only then will the cut-off matrix elements as described above be correct.

CHAPTER 3

APPLICATION OF THE MODIFIED OPW METHOD; BAND STRUCTURE OF NIOBIUM

The modified OPW method described in the preceding chapter has been applied to the transition metal niobium. The details of this application and the resulting band structure are now presented.

The lattice structure of niobium is body-centred cubic. The lattice constant has been taken, after Wyckoff (W48), to be 3.30Å. The first Brillouin zone for the bcc structure is shown in Fig. 3, with the symmetry points and lines labelled in the notation of Bouckaert, Smoluchowski and Wigner (BSW36).

The Potential

A one-body potential used to calculate the conduction electron states should contain the following contributions:

the direct potential contribution from the ion cores;

the self-consistent direct potential of the conduction electrons;

the exchange interaction between the conduction and core electrons;

the correlation interaction between the conduction and core electrons;

the exchange and correlation interactions among the conduction electrons;

spin orbit coupling and other relativistic effects. It is uncertain how to appropriately treat the exchange and correlation interactions. Instead of considering each contribution in detail, the prescription used by Mattheiss (M64) and other authors in APW calculations is adopted. In this approximation free atom charge densities placed on neighboring lattice sites are considered to overlap: The direct potential contributions are then spherically averaged, the core-conduction and conduction-conduction exchange interactions are represented by the Slater free electron approximation and correlation and relativistic effects are ignored. This approach has been found to yield reasonable results when applied by Mattheiss in APW calculations for the first transition series. The procedure is now described.

The charge density used is calculated from the free atom wave functions computed by Herman and Skillman (HS63) in the Hartree-Fock-Slater approximation. The direct and exchange contributions are treated separately. An approximate crystal direct potential and charge density in a given cell is obtained by expanding the neutral atom direct potentials and charge densities of neighboring atoms about the

origin, using Löwdin's alpha function expansion (Lö56), keeping only the ℓ=o terms in these expansions. The exchange potential is taken in the Slater free-electron approximation to be proportional to the cube root of the overlapped charge density.

Let $P^a_{n\ell}$ denote the Herman and Skillman free atom wave functions for Nb. Then the (sperhically averaged) atomic charge density, ρ^a, is given by:

$$\rho^a(r) = \frac{\sigma(r)}{4\pi r^2}$$

where $$\sigma(r) = - \sum_{n\ell} W_{n\ell} \left(P^a_{n\ell}(r)\right)^2$$

and $W_{n\ell}$ is the occupation number for the orbital $n\ell$. (Note that $W_{n\ell} = 2(2\ell+1)$ for the closed shells, 4 for the 4d shell and 1 for the 5s.) The direct atomic potential, $V_d{}^a$, is then

$$V_d{}^a = - \frac{2Z}{r} - \frac{2}{r} \int_o^r \sigma(t)dt - 2 \int_r^\infty \frac{\sigma(t)dt}{t}$$

These direct contributions are then superimposed and spherically averaged to give the crystal direct potential, V_d. The charge densities $\rho^a(r)$ are similarly superimposed and spherically averaged to give the crystal charge density $\rho(r)$. The crystal exchange potential is taken to be $Vex = -6 \left(- \frac{3}{8\pi} \rho(r)\right)^{1/3}$. The total crystal potential, $V(\vec{r})$,

is then defined as:

$$V(\vec{r}) = \sum_{\ell} V_{at}\ (|\overrightarrow{r-R_{\ell}}|)$$

where

$$V_{at}(r) = \begin{cases} V_d + Vex - c & \text{for } o \leq r \leq r_{\ell} \\ o & \text{for } r_{\ell} < r \end{cases}$$

where r_{ℓ} is half the nearest neighbor distance, the constant c is chosen so that $V_{at}(r)$ vanishes at $r=r_{\ell}$ and, as in the preceding chapters, the subscript "at" is to be read "atomic-like".

The resultant $r\ V_{at}(r)$ is listed in Table 3. A Herman and Skillman mesh (HS63) has been used; Table 3 lists the value at each fourth mesh point only. (This potential includes the overlap from the first five sets of neighbors.)

This form of the potential was chosen mainly because it is a simple prescription which has lead to reasonable results in other transition metal band structure calculations. Relativistic effects were ignored to simplify the calculations, particularly in view of the fact that the principal object of this work has been to modify the OPW method. (The effect of relativistic corrections is mentioned later in this chapter, in the section "Discussion of Band Structure Results".) Of course it is to be remembered that, in theory, a self-consistent band structure calculation should be made; a potential constructed as above would provide a suitable starting point in such a calculation.

Since the general features of band structure calculations have usually been found to be relatively insensitive to small changes in the potential, it would appear that the approximations made in constructing this potential are reasonable. However, as discussed later in this chapter (see "Discussion of Band Structure Results"), the Fermi level in the group V transition metals lies in a position such that relatively small changes in the band structure can lead to large variations in the shape of the Fermi surface. The dependence of the Fermi surface on the potential is, then, quite sensitive.

The Core and Cut-Off Functions

The bound state solutions of the atomic-like problem with the potential $V_{at}(r)$ have been found; the energy levels are listed in Table 4. The 4s and 4p functions have been cut off as shown in Figs. 2(a) and 2(b); the dotted lines represent the tail portion of the function before cut-off, while the solid lines represent the cut-off function after orthogonalization to lower core states. The cut-off parameters, as discussed in the preceding chapter, are given in Table 5. It was found that there is no bound state solution corresponding to the atomic 4d level for this potential, so the radial Schrödinger equation was integrated for $\ell=2$ and E= +1.25 rydbergs; this energy was chosen because the resulting wave function was qualitatively of the

desired form. (Of course, the wave function near the core is insensitive to small changes in energy.) The 4d-like cut-off function is plotted in Fig. 2(c).

The Band Structure Program

A band structure program for a Bravais lattice using the modified OPW method has been written in Fortran for the McMaster University IBM 7040 computer. The input data to this program consists of:

the r-mesh and mesh parameters;

the volume of the unit cell;

the potential $V_{at}(r)$;

the values n, ℓ, $E_{n\ell}$ and the functions $P_{n\ell}$ for the completely localized (inner) core states;

the values n, ℓ, $E^{co}_{n\ell}$ and the functions $P^{co}_{n\ell}$ and $G^{co}_{n\ell}$ for the cut-off functions;

the value of the wave vector, $\vec{k}$, in the first Brillouin zone;

the reciprocal lattice vectors, $\vec{G}$, for which the OPW's of wave vector $\vec{k+G}$ are to be used;

the symmetrized combinations of OPW's to be formed for the specific band level concerned;

the required real angular wave functions of the cut-off functions and the lattice harmonic combinations of these which are to be formed.

The program first calculates the orthogonality

coefficients, $F_{n\ell}(k)$, the potential Fourier transforms, $v(G)$, and then the matrix elements given by equations (1-12), (2-10) and (2-12). This (unsymmetrized) matrix is then reduced by taking the lattice harmonic combinations of the real angular wave functions and the symmetrized combinations of OPW's and forming the matrix elements between these linear combinations. The matrix equation (1-7a) is then solved by the following technique:

$$\left[[H] - W [S] \right] \left[a \right] = o \qquad (2\text{-}7a)$$

Multiply on the left by the inverse of $[S]$:

$$\left[\left[S^{-1} \right] [H] - W [I] \right] \left[a \right] = o$$

where $[I]$ denotes the unit matrix. This is now a simple eigenvalue problem for the (non-symmetric) matrix $\left[S^{-1} H \right]$. (The inverted matrix and the eigenvalues are found by the McMaster computer library subroutines.)

Convergence

The objective has been to attain convergence of the band structure to 0.01 rydbergs. The maximum possible number of OPW's have been included subject to the conditions that the dimension of the unsymmetrized matrix not exceed 200 and the dimension of the symmetrized matrix not exceed 50. This means that in most cases 150 to 200 OPW's have been included. Of course these conditions simply reflect

computer time and storage restrictions.

Tables 6 show the degree of convergence at a few typical points: Table 6(a) lists the two lowest solutions of the secular equation as more OPW's are added to the basis set for Γ_1,an s-like combination. The lowest root, -3.106 ry, is the 4s outer core level, which is a narrow band arising from the 4s atomic-like solution which, from Table 4, has an energy of -3.092 ry. The second lowest solution, 0.318 ry, is the bottom of the conduction band. The convergence of these two levels appears to be complete to the number of significant figures shown. Table 6(b) is a similar listing for H_{15}, a p-like combination. The lowest root, -1.517 ry, arises from the 4p atomic-like solution of energy -1.498 ry. The second lowest root is the desired conduction band solution. Tables 6(c) and 6(d) list the results for the d-like combinations Γ_{25}, and Δ_2, the latter shown at $\vec{k}=\frac{2\pi}{a}$ $(\frac{1}{2},0,0)$, the halfway point of the Δ line. At first sight the level Δ_2 might appear to be completely converged since the root does not change in the third decimal point as 168 to 196 OPW's are included. However, this can obviously be misleading, since the same situation occurs as 84 to 116 OPW's are included and yet the level drops by almost 0.01 ry from 116 to 168 OPW's. Perhaps all that can be said about the d-levels is that they might lower by a further 0.02 to 0.03 ry if an infinite

number of OPW's were included, although it is probable that they are better converged than that. In this worst case the d-band levels relative to each other would be correct to the desired accuracy of 0.01 ry but, if the s-band is as fully converged as it appears, then the s-d band gap at Γ, for instance, would be in error by 0.02 to 0.03 ry. The p-band convergence appears to be similar to that of the d-band. (Better convergence for the higher bands, including the p-like levels, could probably be obtained by including 5s, 5p and 5d cut-off functions in the basis set.)

The Band Structure

The band structure has been computed at the points Γ, H, P and N and along the lines Δ, Λ and Σ. The results are listed in Table 7; the roots corresponding to the outer core solutions have been omitted and only those energy values which lie below 1.600 ry (that is, within 1.282 ry of the bottom of the conduction band) have been tabulated. These bands are also plotted in Figs. 4(a), (b) and (c). As discussed in the next section, the Fermi level is expected to lie slightly below $\Gamma_{25'}$.

Discussion of Band Structure Results

Non-relativistic APW band structure calculations have been done for the following bcc transition metals. In the first transition series: bcc iron, $(3d)^6\ (4s)^2$;

vanadium, $(3d)^4\ (4s)^1$; chromium, $(3d)^5\ (4s)^1$; in the third transition series: tungsten, $(5d)^5\ (6s)^1$. The iron calculation was done by Wood (Wo62) along all the symmetry directions and at several general points. He also calculated the corresponding density of states. The potential used was one previously employed in cellular calculations. The vanadium and chromium calculations were performed by Mattheiss (M64) along the Δ direction only. The potential was constructed in the same manner as the present niobium potential except that the constant value of the potential outside the APW sphere was taken to be slightly different from the value at the sphere radius. The results were not sufficiently complete to permit a density of states computation. The tungsten calculation also was done by Mattheiss (M65); it was sufficiently complete to permit a calculation of the density of states. The prescription for the potential was the same as that used in the vanadium and chromium calculations. In addition, a limited APW calculation was done by Mattheiss for the second transition series metal molybdenum, $(4d)^5\ (5s)^1$, to determine the d bandwidth (M65).

The results of the above band structure calculations have been compared by Mattheiss (M65); they have been found to be very similar. The most notable change is an increase in the d bandwidth from the first to the third transition series: $\Delta_d \equiv E(H_{25'}) - E(H_{12})$ is taken as a measure of the d bandwidth. Mattheiss' results are that chromium,

molybdenum and tungsten have d bandwidths of 0.51, 0.68 and 0.77 rydbergs respectively. This progressive increase is expected from tight-binding theory because the 3d, 4d and 5d free atom radial wave functions extend out progressively further so that the overlap of the functions on neighboring sites is progressively greater; this is clear, for instance, from the Hartree-Fock-Slater free atom wave functions of Herman and Skillman (HS63).

The tungsten band structure is compared with the present niobium results in Figs. 6: The solid lines are the niobium results as presented in Figs.4 and the dotted lines are the tungsten bands. The degree of similarity is evident. The d bandwidth, Δ_d, is 0.67 ry, which fits well into the bandwidth pattern discussed above.

Because of the similarity among the bcc transition metal calculations it is useful to assume a rigid band model: In this case, the density of states for these metals is approximated by the density of states which has been calculated for iron or for tungsten. The Fermi level is then determined by filling these states with the required number of conduction electrons. This has been done by Mattheiss for five and six conduction electrons, (M65), corresponding to, respectively, the group V metals vanadium, niobium and tantalum and the group VI metals chromium, molybdenum and tungsten: Using the rigid band approximation, Mattheiss has calculated the Fermi level and presented cross-sections of

the Fermi surface for the group V and group VI cases, both based on the iron and on the tungsten band structures. Mattheiss has found that the Fermi level for the group V metals lies slightly below $\Gamma_{25'}$, and he has computed the shape of the Fermi surface on this basis. It is pointed out by him, however, that a small change in the band structure might lead to a vastly different Fermi surface. Thus, although the band structure itself may be relatively insensitive to a change in the potential (or to the effect of relativistic corrections), the shape of the Fermi surface may alter considerably. This question can only be answered by a self-consistent band structure calculation or by experimental determinations of the Fermi surface. (Experimental data for the group V transition metals is limited due to the lack of pure single crystals.)

No relativistic corrections have been made to the niobium band structure. The nature of spin-orbit coupling corrections is clear from Mattheiss' treatment for tungsten(M65). The results both of a relativistic APW calculation for tungsten by Loucks (Lo65) and the spin-orbit coupling corrections by Mattheiss show, for example, that the relativistic splitting of the $\Gamma_{25'}$ level in tungsten is less than 0.03 ry; of course, it is expected to be less for niobium, which has atomic number 41 compared to Z=74 for tungsten.

The present calculation for niobium tends to confirm the validity of the rigid band approximation for the bcc transition metals. Because of the close similarity to the tungsten results, the density of states and Fermi surface of niobium that would follow from the present calculations are probably well approximated by the group V calculation based on tungsten. It is to be emphasized, however, that both the inaccuracy in the potential and relativistic corrections could be causes of disagreement between the above Fermi surface predictions and future experimental Fermi surface measurements.

Low Order Approximation

In Fig. 5 the energies for the case in which only one symmetrized combination of OPW's is used are shown in dotted lines for three Σ bands. The converged values for these bands, as shown in Fig. 4(c), are reproduced in Fig. 5 in solid lines for the purpose of comparison. In the dotted line results the basis set consists of the cut-off functions plus one symmetrized combination of OPW's, and a secular equation of order 2 or more (depending on the number of lattice harmonic combinations of cut-off functions) is solved at each point in the band.

The error in this low order approximation is seen to be a maximum of about 0.2 ry for the occupied bands. This is an order of magnitude worse than the one-OPW approximation in simple metals: From Heine's results for aluminum (He57), the one-OPW approximation gives a result within

0.03 ry of the converged value. On the other hand, this low order approximation is a considerable improvement over the one-OPW approximation for transition metals: For example, at $\vec{k}$ = (1/4, 1/4, 0) on the Σ_2 band for niobium the one-OPW energy would be 1.3 ry, the low order approximation (cut-off + OPW's) is 0.75 and the converged value is 0.68.

This approximation for the wave functions is obtained by computing the matrix elements between the lattice harmonic combinations of the cut-off functions and the first symmetrized combination of OPW's for the band under consideration, solving the resulting secular equation for its eigenvalues and eigenvectors. The eigenvectors denote the amount of admixture between the cut-off functions and the OPW's. These eigenvectors for the three Σ bands of Fig. 5 are listed in Table 8: a_ℓ denotes the coefficient of a cut-off function with angular momentum ℓ, and b denotes the coefficient of the first symmetrized combination of OPW's. The normalization of the eigenvectors is chosen so that b=1.00 in all cases. As an example, for the case of Σ_2 the only cut-off function to be used is the d function with the lattice harmonic combination (ℓmj) = (211) + (210) (see Table 2). Denote this function by ϕ^{CO} and the first symmetrized combination of OPW's by $\phi^{OPW}(\vec{k})$. The solution is of the form:

$$a_d \phi^{CO} + b\phi^{OPW}(\vec{k})$$

From Table 8, the coefficients a_d and b for k = (1/4,1/4,0) are 7.03 and 1.00 respectively. (Note that for the Σ_1 band an s, p and two d lattice harmonic combinations of cut-off functions are to be used (see Table 2).)

For a band having a symmetry which is dominantly of one spherical harmonic component throughout the band it is expected that the admixture of cut-off and OPW functions will be relatively constant across the band. This is predicted on physical grounds since in such a case the wave function near the core will not change appreciably as the energy changes across a band, and the cut-off function represents the wave function near the core. The band Σ_2 is of this type. Although, from Table 8, the coefficients a_d take on the values 7.96, 7.03 and 6.56 at three consecutive points along the band, the effect of this variation of coefficients on the energy is very small: A calculation has been done for this band in which the coefficients at $\vec{k}$ = (1/4, 1/4, 0) (that is, from Table 8, a_d=7.03 and b=1.00) have been used at the points $\vec{k}$ = (1/8, 1/8, 0) and (3/8, 3/8, 0). At both points the expectation value of the energy for this combination agreed to within 0.01 ry with the result using the correct coefficients of Table 8.

It should be emphasized that the primary purpose of the present work has been a complete band structure calculation and the above is a low order approximation which is present in this modified OPW method. If the interest is

especially in a simple approximation to the wave functions there are two obvious improvements to be made to the above approach: First, a tight-binding combination of the d atomic states could be used instead of the d cut-off function; although numerical approximations would have to be made in computing the matrix elements between the tight-binding function and the OPW's, the d bands would probably be better represented. Secondly, there would be no need to use cut-off s and p functions; the plane waves could be orthogonalized to the outer core functions in an approximate way.

CONCLUSION

The OPW method has been successfully modified to permit band structure calculations in transition metals. The rate of convergence leaves something to be desired; this disadvantage is felt mainly in computation time. The band structure of niobium computed by this method is similar to APW calculations in other bcc transition metals, comfirming the validity of a rigid band approximation. It is still an open question whether a modified OPW method, the APW method or some other approach will prove most successful in the self-consistent band structure calculations which will probably be performed in the near future.

A secondary result is a first principle low order approximation to the wave functions in transition metals. Although its error is in the range of 10% to 20% it may be a step in the direction of more accurate approximations.

In summary, it is believed that this work provides a proven alternative to the augmented plane wave approach and also opens up the possibility of applications in which the conduction electrons in transition metals are represented in a relatively simple way.

CAPTIONS FOR FIGURES

Fig. 1 Fourier transforms of the attractive and effective repulsive potentials for Si after Phillips and Kleinman (PK59).

(a) s-like point

(b) p-like point

Fig. 2 The radial cut-off functions, $P^{co}_{n\ell}$.

(a) 4s

(b) 4p

(c) 4d

Fig. 3 Brillouin zone for the body-centred cubic lattice.

Fig. 4 Energy bands in niobium.

Fig. 5 The low order approximation (dotted lines) is compared with the converged results (solid lines) for three Σ bands.

Fig. 6 APW energy bands in tungsten (dotted lines), after Mattheiss (M65) are compared to the niobium bands.

FIG I(a)

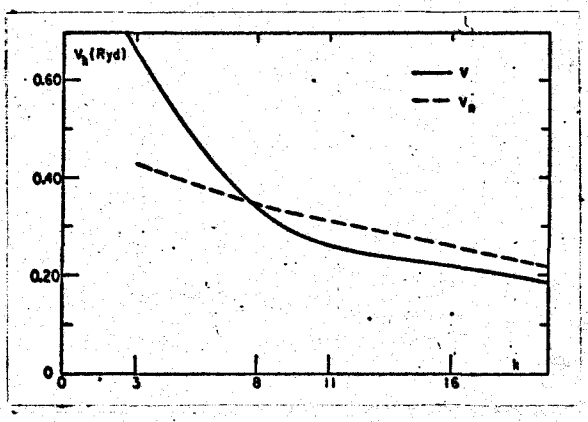

FIG I(b)

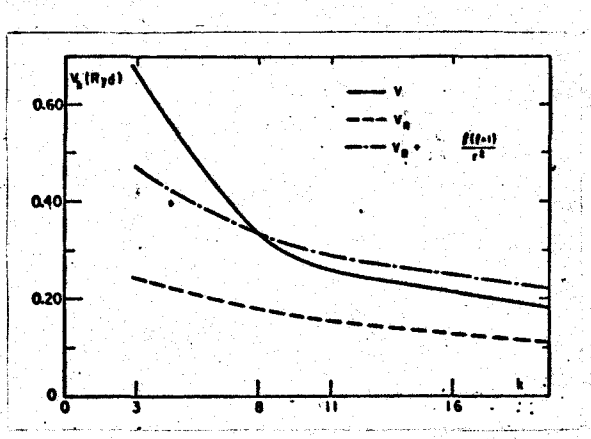

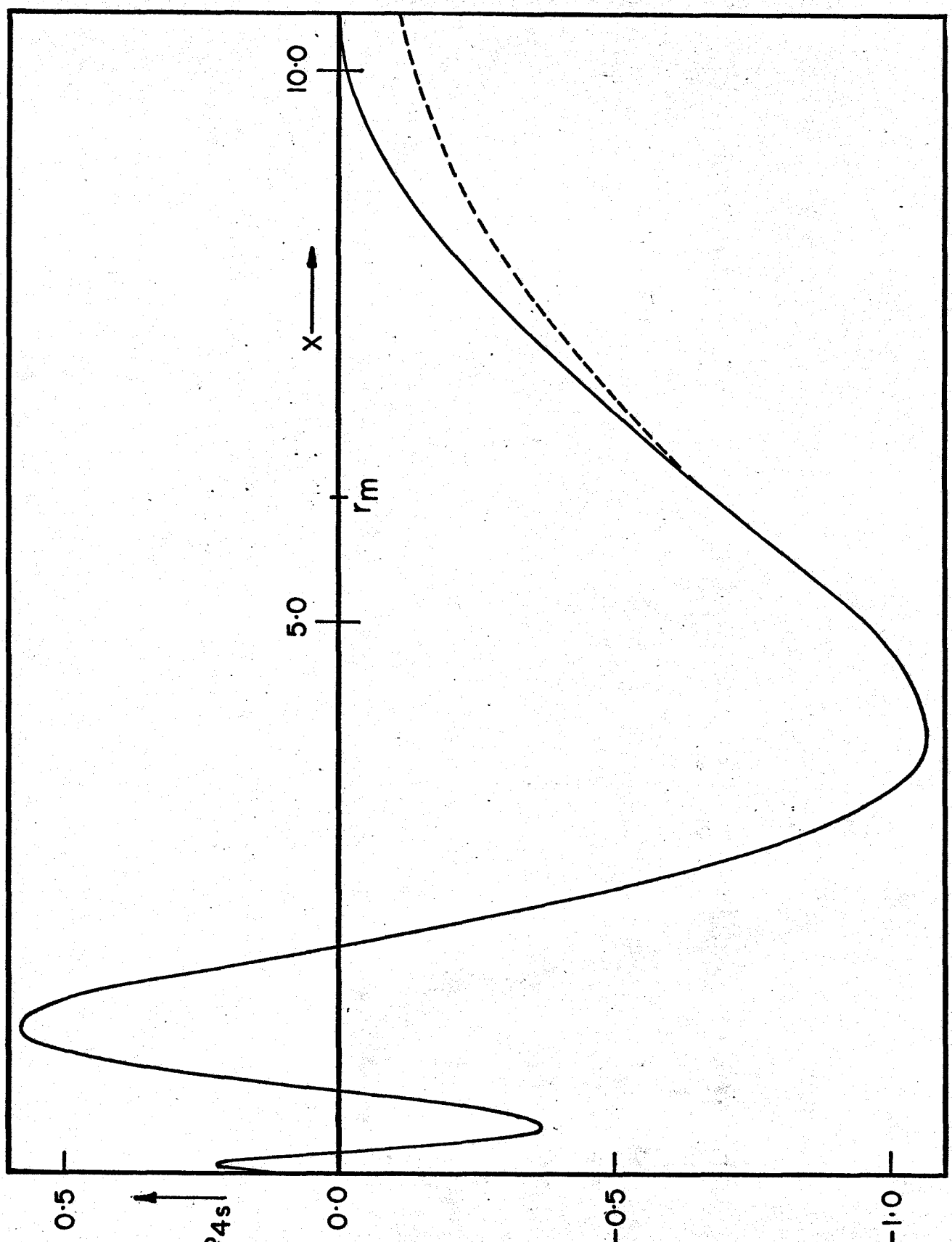

FIG 2(a)

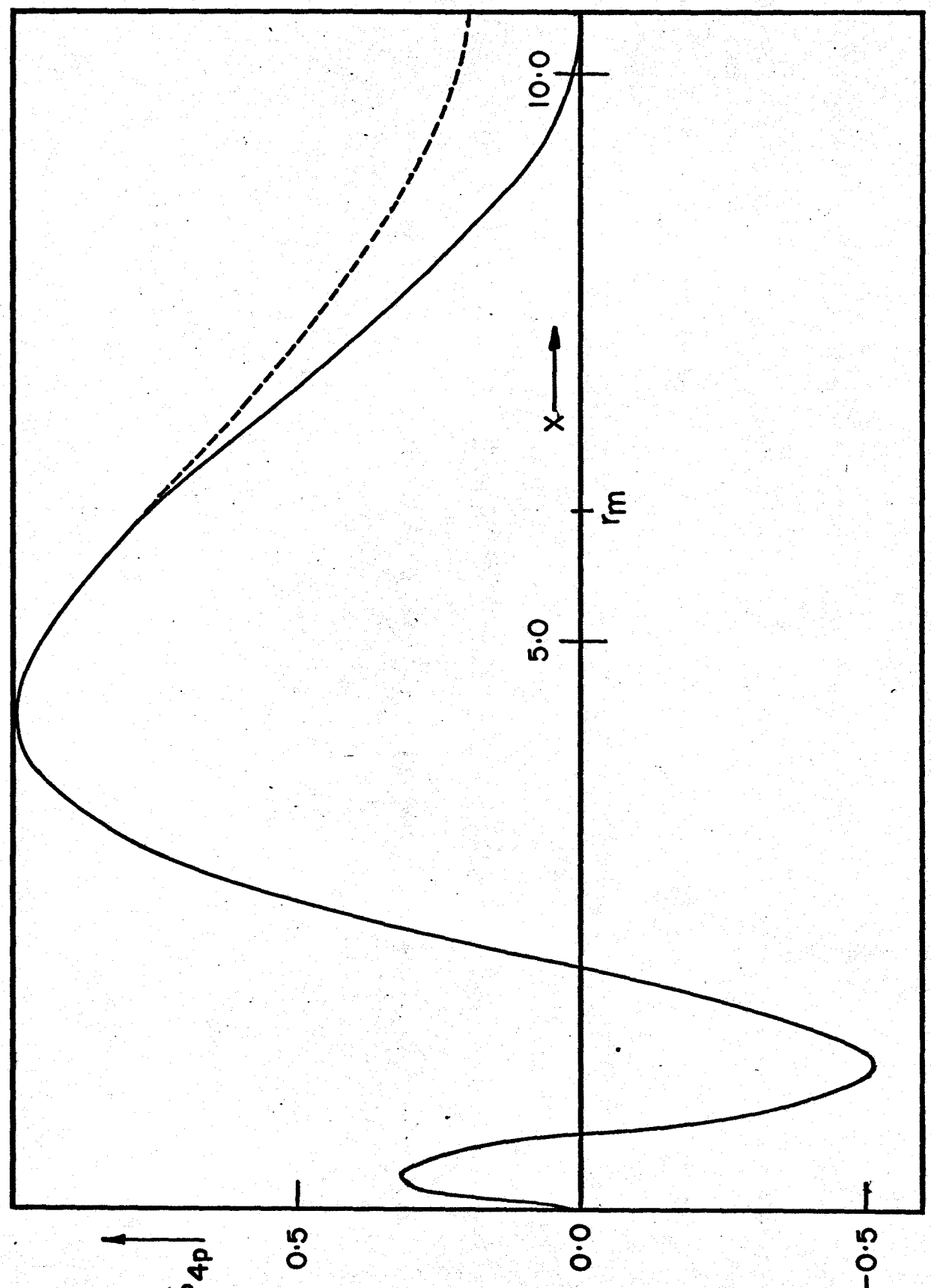

FIG 2(b)

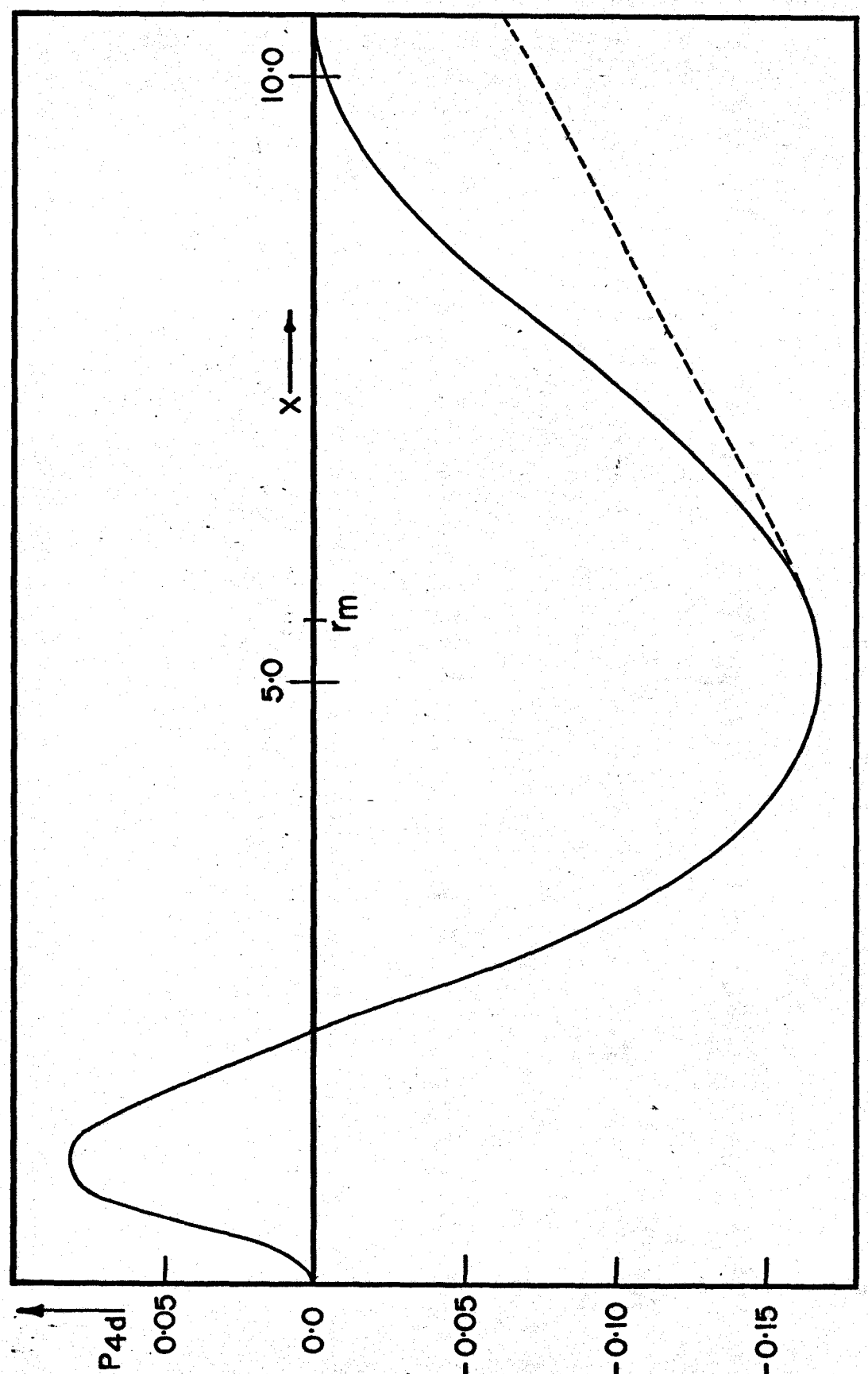

FIG 2(c)

FIG 3

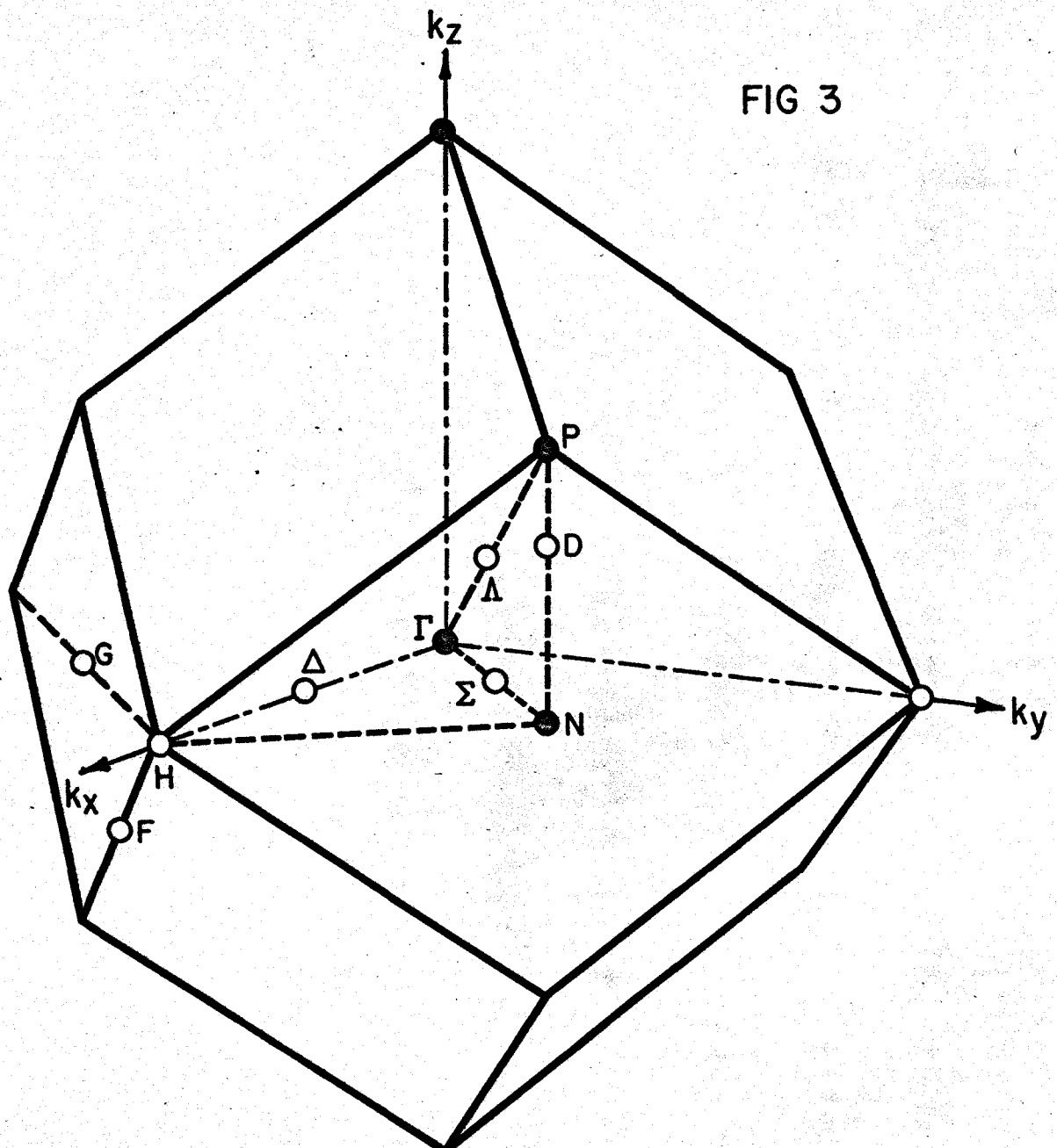

FIG 4 (a)

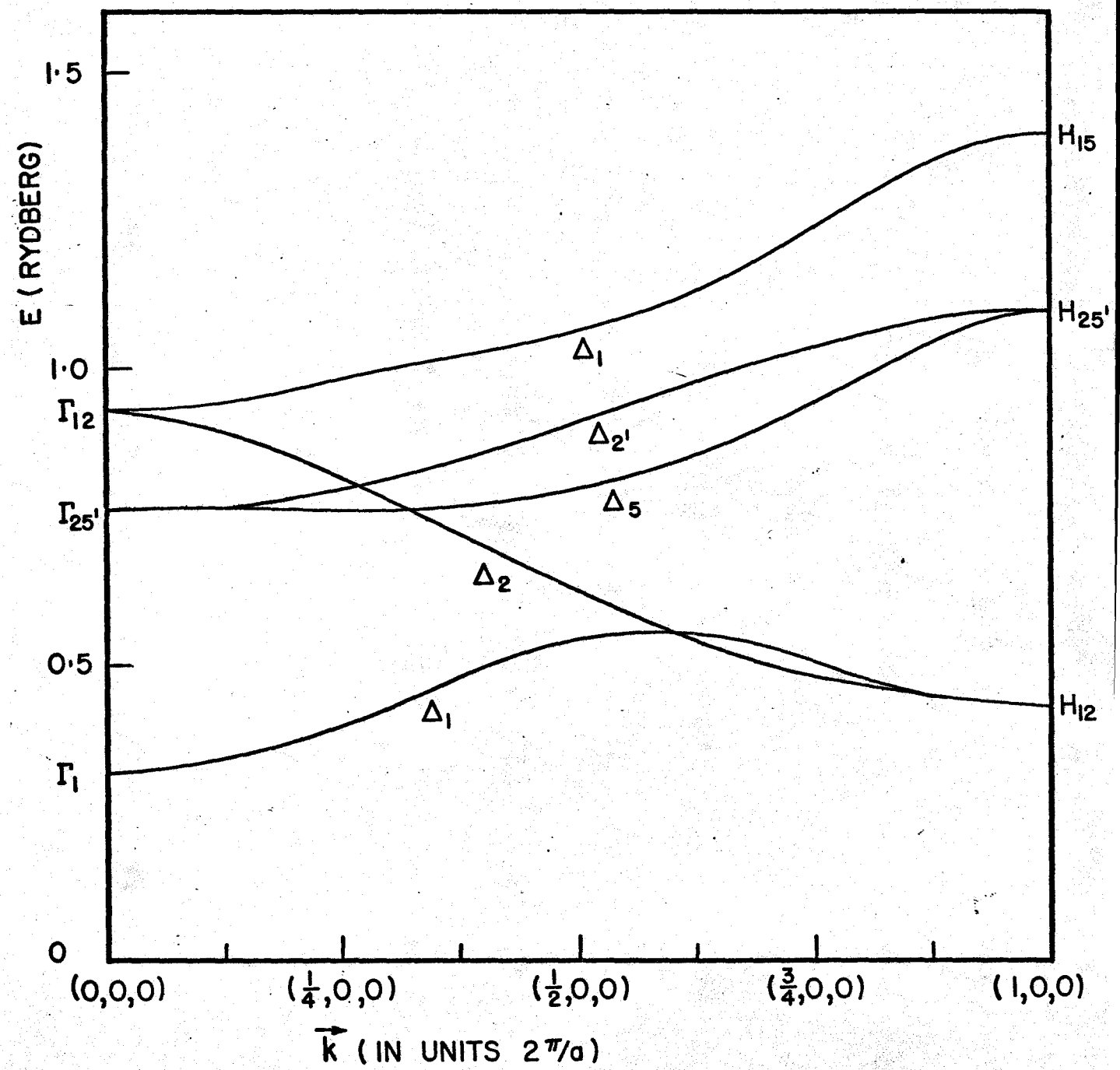
1·5
1·0
0·5
0
E (RYDBERG)
Γ_{12}
$\Gamma_{25'}$
Γ_1
H_{15}
$H_{25'}$
H_{12}
Δ_1
$\Delta_{2'}$
Δ_5
Δ_2
Δ_1
(0,0,0)
$(\frac{1}{4},0,0)$
$(\frac{1}{2},0,0)$
$(\frac{3}{4},0,0)$
(1,0,0)
$\vec{k}$ (IN UNITS $2\pi/a$)

FIG 4 (b)

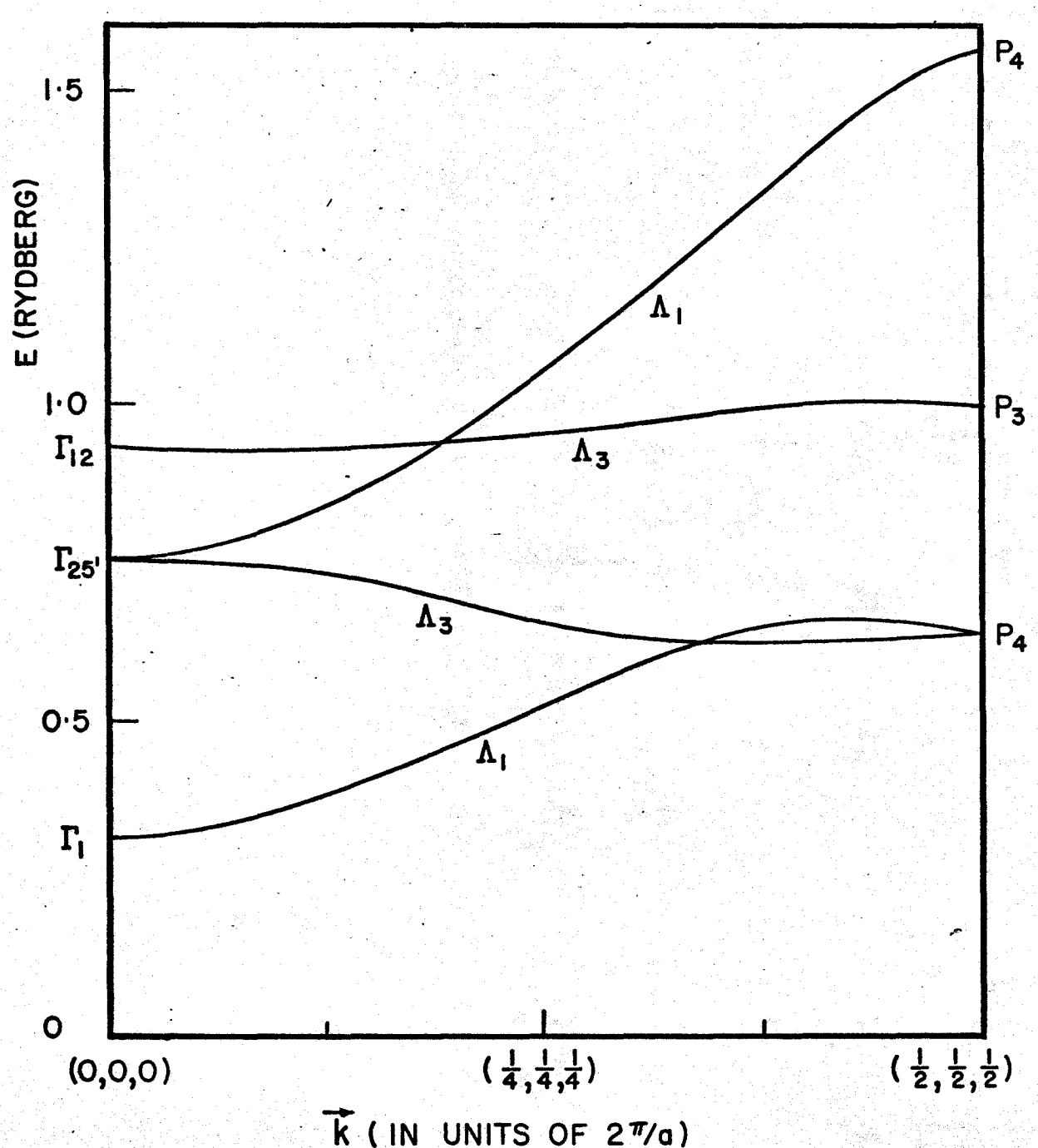
E (RYDBERG)
1·5
1·0
0·5
0
Γ_{12}
$\Gamma_{25'}$
Γ_1
Λ_1
Λ_3
Λ_3
Λ_1
P_4
P_3
P_4
(0,0,0)
$(\frac{1}{4},\frac{1}{4},\frac{1}{4})$
$(\frac{1}{2},\frac{1}{2},\frac{1}{2})$
$\vec{k}$ (IN UNITS OF $2\pi/a$)

FIG 4(c)

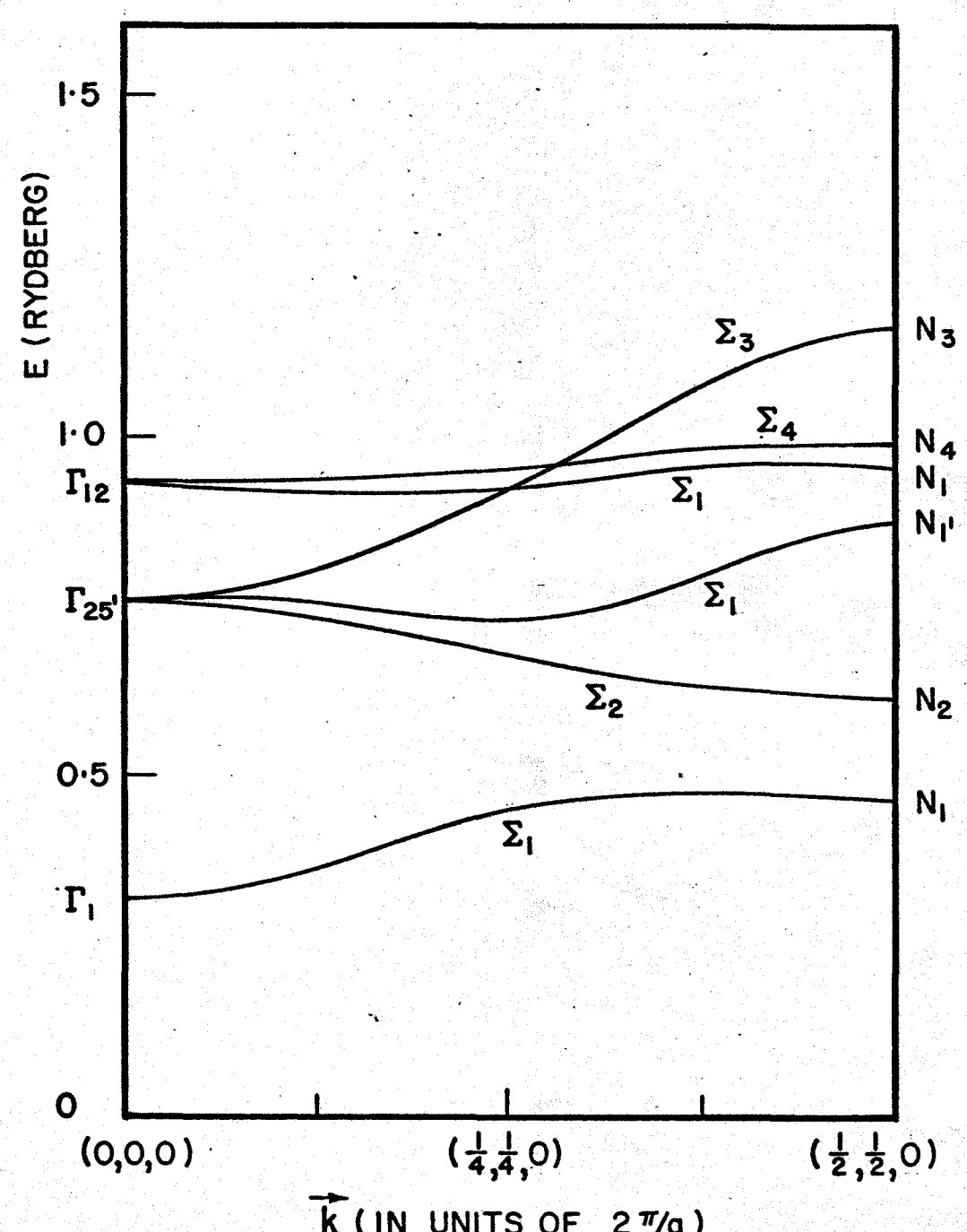
1·5
1·0
0·5
0
E (RYDBERG)
Γ12
Γ25'
Γ1
Σ3
Σ4
Σ1
Σ1
Σ2
Σ1
N3
N4
N1
N1'
N2
N1
(0,0,0)
(¼,¼,0)
(½,½,0)
k (IN UNITS OF 2π/a)

FIG 5

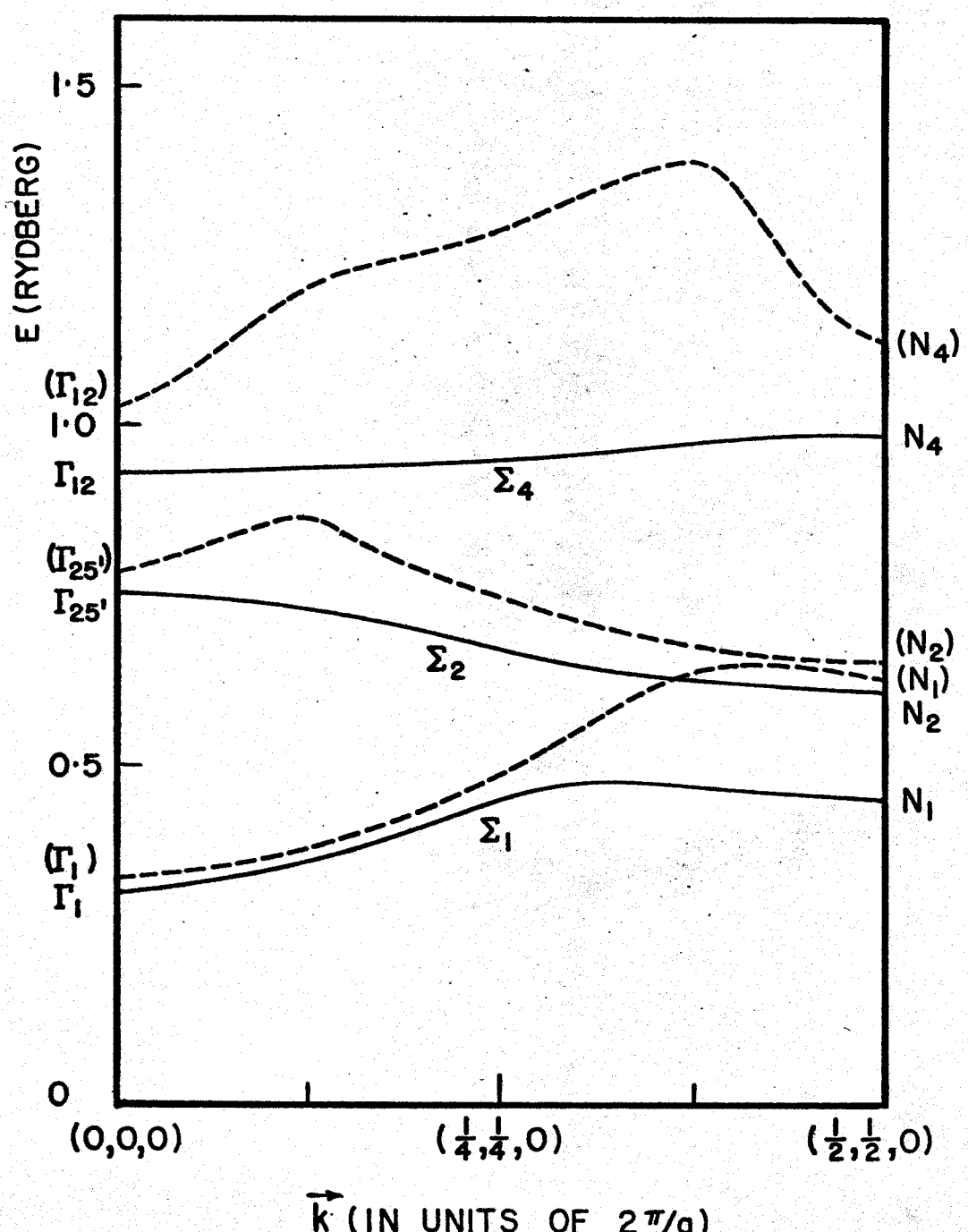
E (RYDBERG)
1·5
1·0
0·5
0
(Γ12)
Γ12
(Γ25')
Γ25'
(Γ1)
Γ1
(N4)
N4
Σ4
(N2)
(N1)
N2
Σ2
N1
Σ1
(0,0,0)
(¼,¼,0)
(½,½,0)
k (IN UNITS OF 2π/a)

FIG 6.(a)

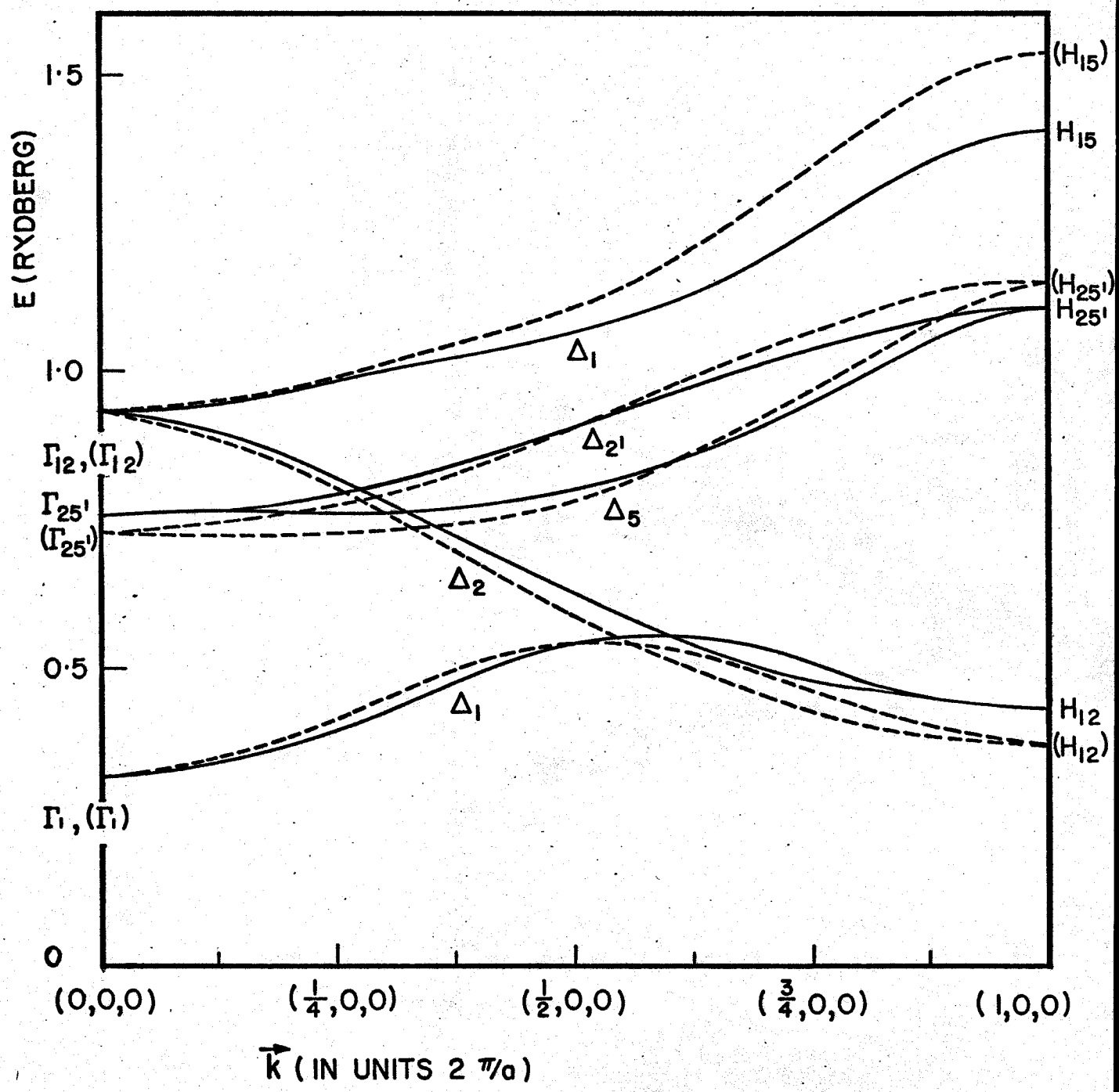
E (RYDBERG)
1·5
1·0
0·5
0
$\Gamma_{12}, (\Gamma_{12})$
$\Gamma_{25'}$
$(\Gamma_{25'})$
$\Gamma_1, (\Gamma_1)$
(H_{15})
H_{15}
$(H_{25'})$
$H_{25'}$
H_{12}
(H_{12})
Δ_1
$\Delta_{2'}$
Δ_5
Δ_2
Δ_1
(0,0,0)
$(\frac{1}{4},0,0)$
$(\frac{1}{2},0,0)$
$(\frac{3}{4},0,0)$
(1,0,0)
$\vec{k}$ (IN UNITS $2\pi/a$)

FIG 6(b)

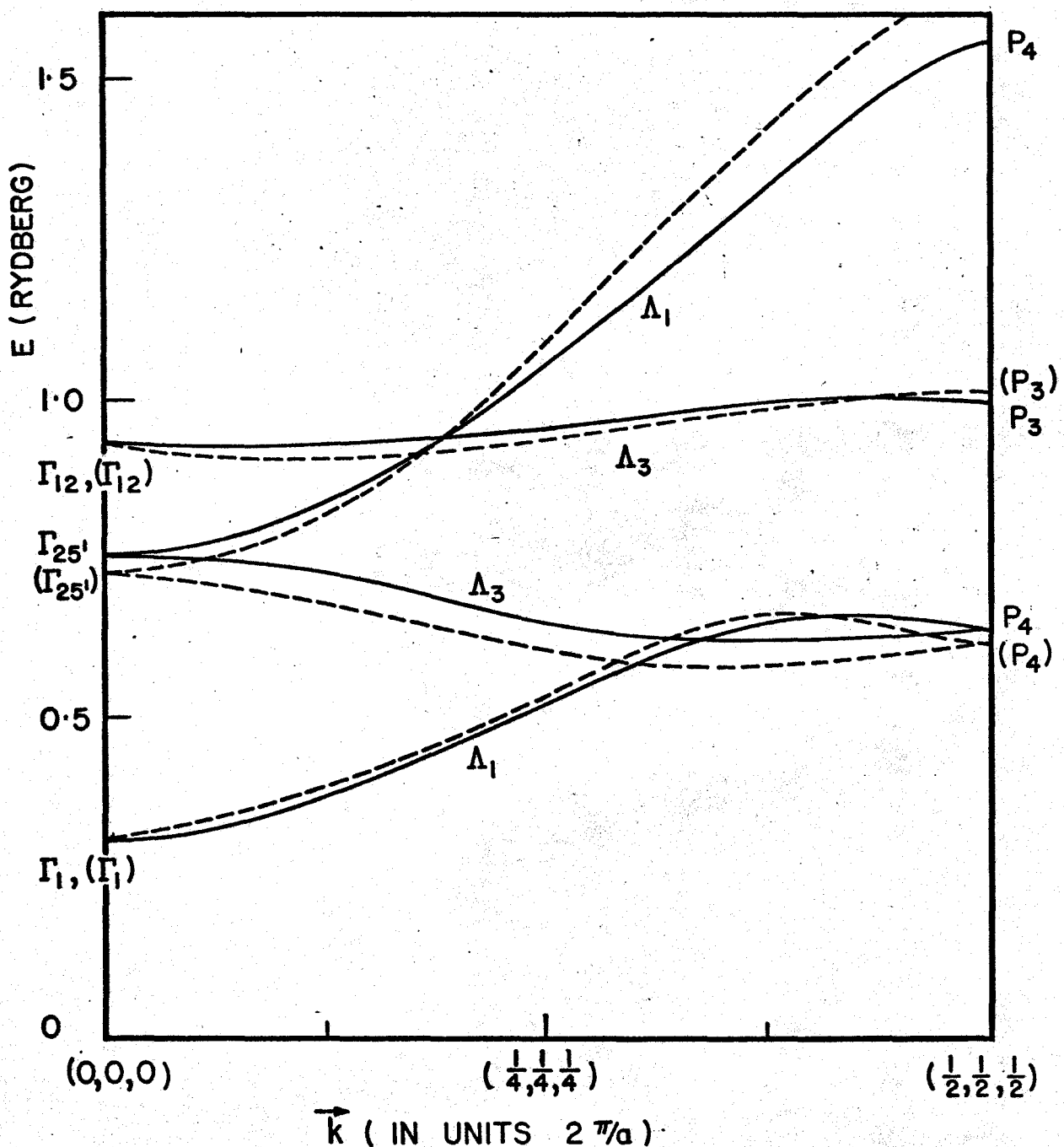
E (RYDBERG)
1·5
1·0
0·5
0
$\Gamma_{12}, (\Gamma_{12})$
$\Gamma_{25'}$
$(\Gamma_{25'})$
$\Gamma_1, (\Gamma_1)$
Λ_1
Λ_3
Λ_3
Λ_1
P_4
(P_3)
P_3
P_4
(P_4)
(0,0,0)
$(\frac{1}{4},\frac{1}{4},\frac{1}{4})$
$(\frac{1}{2},\frac{1}{2},\frac{1}{2})$
$\vec{k}$ (IN UNITS $2\pi/a$)

FIG 6(c)

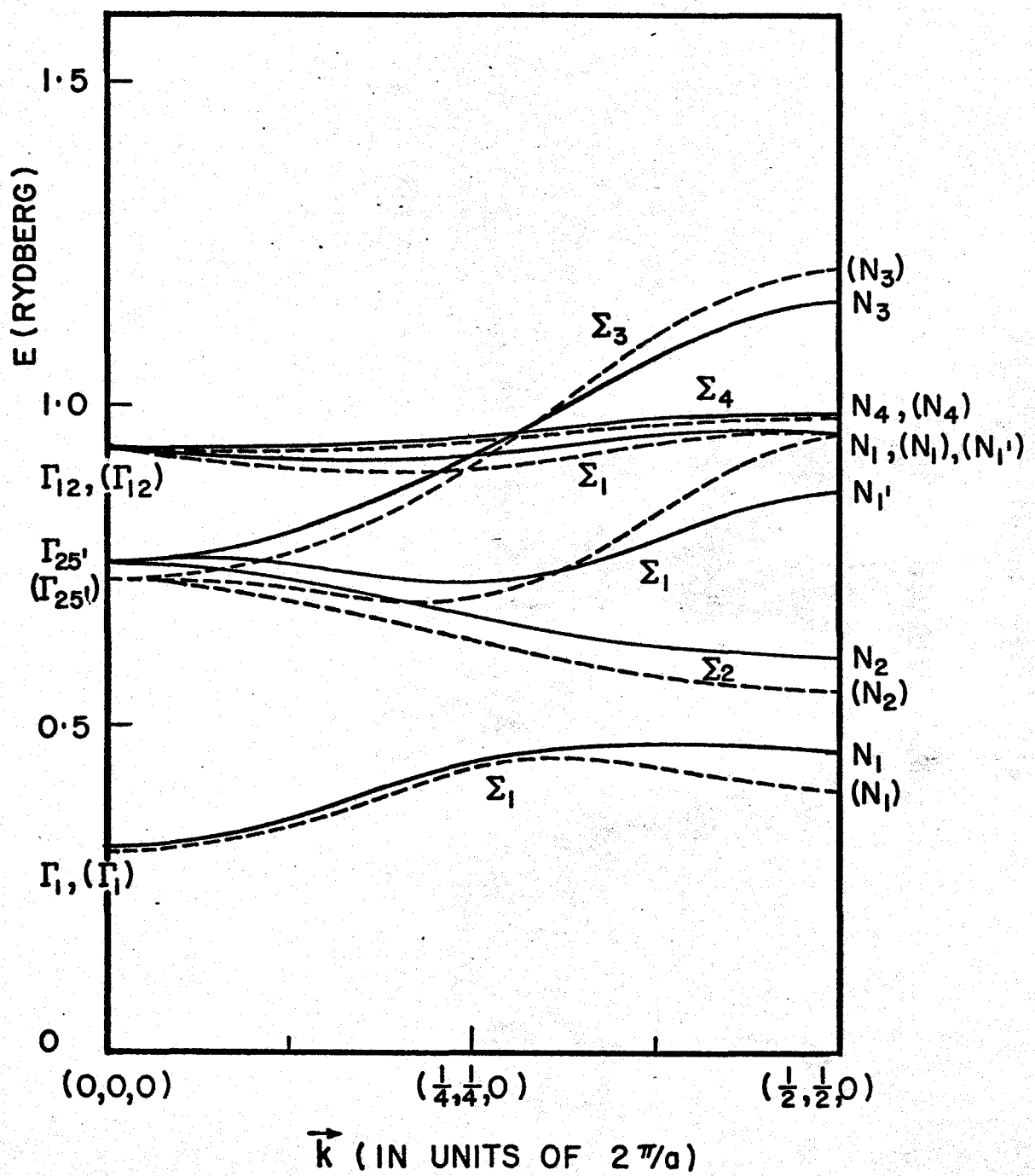
1·5
1·0
0·5
0
E (RYDBERG)
$\Gamma_{12}, (\Gamma_{12})$
$\Gamma_{25'}$
$(\Gamma_{25'})$
$\Gamma_1, (\Gamma_1)$
Σ_3
Σ_4
Σ_1
Σ_1
Σ_2
Σ_1
(N_3)
N_3
$N_4, (N_4)$
$N_1, (N_1), (N_{1'})$
$N_{1'}$
N_2
(N_2)
N_1
(N_1)
(0,0,0)
$(\frac{1}{4},\frac{1}{4},0)$
$(\frac{1}{2},\frac{1}{2},0)$
$\vec{k}$ (IN UNITS OF $2\pi/a$)

TABLE 1

REAL ANGULAR WAVE FUNCTIONS $y_{\ell mj}$

(ℓmj)	$y_{\ell mj}$
(000)	$\frac{1}{\sqrt{4\pi}}$
(100)	$\sqrt{\frac{3}{4\pi}}\ \frac{z}{r}$
(110)	$-\sqrt{\frac{3}{4\pi}}\ \frac{y}{r}$
(111)	$\sqrt{\frac{3}{4\pi}}\ \frac{x}{r}$
(200)	$\sqrt{\frac{5}{4\pi}}\ \frac{z^2-\frac{1}{2}(x^2+y^2)}{r^2}$
(210)	$-\sqrt{\frac{15}{4\pi}}\ \frac{yz}{r^2}$
(211)	$\sqrt{\frac{15}{4\pi}}\ \frac{xz}{r^2}$
(220)	$-\sqrt{\frac{15}{16\pi}}\ \frac{(x^2-y^2)}{r^2}$
(221)	$-\sqrt{\frac{15}{4\pi}}\ \frac{xy}{r^2}$

TABLE 2

LATTICE HARMONICS IN TERMS OF THE REAL ANGULAR WAVE FUNCTIONS OF TABLE 1. COLUMN 1 SHOWS THE BSW NOTATION; COLUMN 2 IS THE NOTATION OF D. G. BELL (B54); COLUMN 3 CONTAINS UNNORMALIZED LATTICE HARMONIC COMBINATIONS OF $\ell \leq 2$ ONLY.

BSW	DGB	LATTICE HARMONICS (ℓmj)
Γ_1 (1)	A_s	(000)
Γ_{15} (x)	A_p	(111)
Γ_{12} (x^2-y^2)	A_d	(220)
Γ_{25}, (yz)	$A_{d'}$	(210)
H	same as Γ	
P_1 (1)	B_s	(000)
P_3 (x^2-y^2)	B_d	(220)
P_4 (x)	B_p	(111), (210)
N_1 (1)	G_s	(000), (200), (221)
N_2 (z(x-y))	$G_{d'}$	(211)+(210)
N_3 (z(x+y))	$G_{d''}$	(211)-(210)
N_4 (x^2-y^2)	G_d	(220)
N_1' (x+y)	$G_{p'}$	(111)-(110)
N_3' (z)	G_p	(100)
N_4' (x-y)	$G_{p''}$	(111)+(110)
Δ_1 (1)	E_s	(000), (111), (200)+$\sqrt{3}$(220)
Δ_2 (y^2-z^2)	$E_{d'}$	(220)-$\sqrt{3}$(200)
Δ_2, (yz)	E_d	(210)
Δ_5 (y)	E_p	(110), (221)
Λ_1 (1)	I_s	(000), (100)+(111)-(110), (211)-(210)-(221)
Λ_3 (x-y)	I_p	(111)+(110), (220), (211)+(210)
Σ_1 (1)	L_s	(000), (111)-(110), (200), (221)
Σ_2 (z(x-y))	L_d	(211)+(210)
Σ_3 (z)	$L_{p'}$	(100), (211)-(210)
Σ_4 (x-y)	L_p	(111)+(110), (220)

TABLE 3

THE ATOMIC-LIKE POTENTIAL AS A FUNCTION OF x,

WHERE r=0.25675x

x	r $V_{at}(r)$	x	r $V_{at}(r)$
0.00	-82.0000	1.10	-33.2288
0.01	-81.1273	1.18	-31.5998
0.02	-80.2358	1.26	-30.0856
0.03	-79.3396	1.34	-28.6767
0.04	-78.4481	1.42	-27.3651
0.05	-77.5670	1.50	-26.1435
0.06	-76.6998	1.66	-23.2930
0.07	-75.8485	1.82	-22.0204
0.08	-75.0137	1.98	-20.3254
0.09	-74.1957	2.14	-18.8158
0.10	-73.3943	2.30	-17.4598
0.12	-71.8392	2.46	-16.2355
0.14	-70.3457	2.62	-15.1284
0.16	-68.9114	2.78	-14.1278
0.18	-67.5350	2.94	-13.2236
0.20	-66.2149	3.10	-12.4039
0.22	-64.9487	3.42	-10.9685
0.24	-63.7328	3.74	- 9.7337
0.26	-62.5628	4.06	- 8.6434
0.28	-61.4342	4.38	- 7.6678
0.30	-60.3431	4.70	- 6.7904
0.34	-58.2605	5.02	- 6.0001
0.38	-56.2955	5.34	- 5.2876
0.42	-54.4355	5.66	- 4.6449
0.46	-52.6711	5.98	- 4.0643
0.50	-50.9944	6.30	- 3.5391
0.54	-49.3982	6.94	- 2.6324
0.58	-47.8761	7.58	- 1.8875
0.62	-46.4229	8.22	- 1.2785
0.66	-45.0343	8.86	- 0.7872
0.70	-43.7070	9.50	- 0.4009
0.78	-41.2258	10.14	- 0.1108
0.86	-38.9603	10.46	0.0000
0.94	-36.8886		
1.02	-34.9857		

TABLE 4

THE BOUND STATE SOLUTIONS OF THE ATOMIC-LIKE POTENTIAL OF TABLE 3

Core	nℓ	$E_{n\ell}$
Inner	1s	-1358.5
	2s	- 187.66
	2p	- 173.03
	3s	- 30.719
	3p	- 25.034
	3d	- 14.519
Outer	4s	- 3.092
	4p	- 1.498

TABLE 5

THE CUT-OFF FUNCTION PARAMETERS

nℓ	$E^{co}_{n\ell}$	r_ℓ	r_m	r_o
4s	-3.092	2.6856	1.5765	0.6571
4p	-1.498	2.6856	1.5765	1.1440
4d	+1.250	2.6856	1.4121	1.3350

TABLE 6(a)

CONVERGENCE OF Γ_1 (s-like)

No. of OPW's	Dimension of Reduced Matrix	Lowest Eigenvalue	Second Lowest Eigenvalue
0	1	-3.018	
1	2	-3.085	0.330
13	3	-3.085	0.328
19	4	-3.089	0.326
43	5	-3.093	0.325
55	6	-3.093	0.325
79	7	-3.100	0.321
87	8	-3.102	0.320
135	9	-3.106	0.318
141	10	-3.106	0.318
153	11	-3.106	0.318
177	12	-3.106	0.318

TABLE 6(b)

CONVERGENCE OF H_{15}(p-like)

No. of OPW's	Dimension of Reduced Matrix	Lowest Eigenvalue	Second Lowest Eigenvalue
0	1	-1.335	
2	2	-1.468	1.479
10	3	-1.473	1.447
26	5	-1.489	1.429
28	6	-1.490	1.424
52	8	-1.495	1.424
76	10	-1.495	1.421
92	12	-1.503	1.415
108	14	-1.507	1.414
132	16	-1.514	1.409
156	18	-1.517	1.406

TABLE 6(c)

CONVERGENCE OF $\Gamma_{25'}$ (d-like)

No. of OPW's	Dimension of Reduced Matrix	Lowest Eigenvalue
0	1	1.486
4	2	0.786
28	4	0.785
32	5	0.781
40	6	0.775
48	7	0.772
96	10	0.770
100	11	0.769
124	13	0.767
132	14	0.764
156	16	0.760
180	18	0.758

TABLE 6(d)

CONVERGENCE OF Δ_2 (d-like) AT $(\frac{1}{2},0,0)\ ^{2\pi}/a$

No. of OPW's	Dimension of Reduced Matrix	Lowest Eigenvalue
0	1	1.486
4	2	0.671
8	3	0.668
12	4	0.655
20	5	0.651
28	6	0.650
32	7	0.648
36	8	0.648
40	9	0.648
44	10	0.647
52	11	0.642
56	12	0.637
60	13	0.637
68	14	0.637
76	15	0.635
84	16	0.634
92	17	0.634
100	18	0.634
108	19	0.634
112	20	0.634
116	21	0.634
124	22	0.633
132	23	0.631
136	24	0.631
140	25	0.631
144	26	0.630
152	27	0.628
156	28	0.628
160	29	0.628
168	30	0.627
176	31	0.627
184	32	0.627
192	33	0.627
196	34	0.627

TABLE 7

CONDUCTION BANDS OF NIOBIUM

Symmetry	$\vec{k}$ Units of $2\pi/a$	No. of OPW's	Lowest Band Root (rydbergs)	Second Lowest	Third Lowest
Γ_1	(0,0,0)	177	0.318		
Γ_{12}	(0,0,0)	192	0.932		
$\Gamma_{25'}$	(0,0,0)	180	0.758		
H_{15}	(1,0,0)	156	1.406		
H_{12}	(1,0,0)	196	0.434		
$H_{25'}$	(1,0,0)	184	1.106		
P_3	(½,½,½)	192	0.998		
P_4	(½,½,½)	192	0.645	1.563	
N_1	(½,½,0)	194	0.460	0.956	
N_2	(½,½,0)	192	0.612		
N_3	(½,½,0)	196	1.159		
N_4	(½,½,0)	192	0.990		
$N_{1'}$	(½,½,0)	198	0.873		
Δ_1	(1/8,0,0)	193	0.340	0.949	
Δ_1	(¼,0,0)	193	0.400	0.982	
Δ_1	(3/8,0,0)	193	0.480	1.025	
Δ_1	(½,0,0)	193	0.543	1.068	
Δ_1	(5/8,0,0)	193	0.551	1.131	
Δ_1	(3/4,0,0)	193	0.507	1.236	
Δ_1	(7/8,0,0)	193	0.458	1.352	
Δ_2	(1/8,0,0)	196	0.900		
Δ_2	(1/4,0,0)	196	0.819		
Δ_2	(3/8,0,0)	196	0.721		
Δ_2	(½,0,0)	196	0.627		
Δ_2	(5/8,0,0)	196	0.546		
Δ_2	(3/4,0,0)	196	0.486		
Δ_2	(7/8,0,0)	196	0.449		
$\Delta_{2'}$	(1/8,0,0)	196	0.768		
$\Delta_{2'}$	(¼,0,0)	196	0.797		
$\Delta_{2'}$	(3/8,0,0)	196	0.844		

/cont'd..

Table 7 (continued)

Symmetry	$\vec{k}$ Units of $2\pi/a$	No. of OPW's	Lowest Band Root (rydbergs)	Second Lowest	Third Lowest
$\Delta_{2'}$	(½,0,0)	196	0.905		
$\Delta_{2'}$	(5/8,0,0)	196	0.974		
$\Delta_{2'}$	(3/4,0,0)	196	1.040		
$\Delta_{2'}$	(7/8,0,0)	196	1.089		
Δ_5	(1/8,0,0)	162	0.762		
Δ_5	(1/4,0,0)	162	0.759		
Δ_5	(3/8,0,0)	162	0.769		
Δ_5	(½,0,0)	162	0.800		
Δ_5	(5/8,0,0)	162	0.860		
Δ_5	(3/4,0,0)	162	0.946		
Δ_5	(7/8,0,0)	162	1.050		
Λ_1	(1/8,1/8,1/8)	189	0.381	0.842	
Λ_1	(1/4,1/4,1/4)	189	0.522	1.059	
Λ_1	(3/8,3/8,3/8)	189	0.652	1.332	
Λ_3	(1/8,1/8,1/8)	126	0.733	0.934	
Λ_3	(1/4,1/4,1/4)	126	0.654	0.959	
Λ_3	(3/8,3/8,3/8)	126	0.623	1.000	
Σ_1	(1/8,1/8,0)	139	0.361	0.758	0.918
Σ_1	(¼,¼,0)	139	0.453	0.722	0.922
Σ_1	(3/8,3/8,0)	139	0.476	0.792	0.959
Σ_2	(1/8,1/8,0)	172	0.733		
Σ_2	(¼,¼,0)	172	0.678		
Σ_2	(3/8,3/8,0)	172	0.632		
Σ_3	(1/8,1/8,0)	174	0.804		
Σ_3	(¼,¼,0)	174	0.922		
Σ_3	(3/8,3/8,0)	174	1.078		
Σ_4	(1/8,1/8,0)	166	0.940		
Σ_4	(¼,¼,0)	166	0.953		
Σ_4	(3/8,3/8,0)	166	0.981		

TABLE 8

TYPICAL EIGENVECTORS FOR THE LOW ORDER APPROXIMATION (CUT-OFF FUNCTIONS + ONE SYMMETRIZED COMBINATION OF OPW'S)

Symmetry	Coefficients	$\vec{k}$-value (1/8,1/8,0)	($\frac{1}{4}$,$\frac{1}{4}$,0)	(3/8,3/8,0)
Σ_1	a_s =	2.35	2.22	2.03
	a_p =	0.466	0.862	1.16
	a_d =	0.186	0.828	2.12
	$a_{d'}$ =	0.322	1.43	3.68
	b =	1.00	1.00	1.00
Σ_2	a_d =	7.96	7.03	6.56
	b =	1.00	1.00	1.00
Σ_4	a_p =	0.690	0.739	0.766
	a_d =	-16.4	-16.5	-20.2
	b =	1.00	1.00	1.00

REFERENCES

B54 D. G. Bell, Rev. Mod. Phys., 26, 311 (1954).

BSW36 L. P. Bouckaert, R. Smoluchowski, E. Wigner, Phys. Rev., 50, 58 (1936).

C55a J. Callaway, Phys. Rev., 97, 933 (1955).

C55b J. Callaway, Phys. Rev., 99, 500 (1955).

G65 S. Golin, Phys. Rev., 140, A993 (1965).

H40 C. Herring, Phys. Rev., 57, 1169 (1940).

Ha66 W. A. Harrison, Pseudopotentials in the Theory of Metals (Benjamin, 1966).

He57 V. Heine, Proc. Royal Soc. A, 240, 340 (1957).

HS63 F. Herman, S. Skillman, Atomic Structure Calculations (Prentice-Hall, 1963).

L66 A. W. Luehrmann, Crystal Symmetries of Plane-Wave-Like Functions (Department of Physics and Institute for the study of Metals, The University of Chicago, 1966).

Lo56 P. O. Löwdin, Advan. Phys., 5, 1 (1956).

Lo65 T. L. Loucks, Phys. Rev. Letters, 14, 693 (1965).

LC64 T. L. Loucks, P. H. Cutler, Phys. Rev., 133, A819 (1964).

M64 L. F. Mattheiss, Phys. Rev., 134, A970 (1964).

M65 L. F. Mattheiss, Phys. Rev., 139, A1893 (1965).

MM43 H. Margenau, G. M. Murphy, The Mathematics of Physics and Chemistry, Sec. 11.20 (Van Nostrand, 1943).

PK59 J. C. Phillips, L. Kleinman, Phys. Rev., 116, 287 (1959).

S62 H. Schlosser, J. Phys. Chem. Solids, 23, 963 (1962).

S165 J. C. Slater, Quantum Theory of Molecules and Solids, Vol. 2, Sec. 9-2 (McGraw-Hill, 1965).

Ti64 M. Tinkham, Group Theory and Quantum Mechanics (McGraw-Hill, 1964).

W48 R. W. G. Wyckoff, Crystal Structures (Interscience, 1948).

Wo62 J. H. Wood, Phys. Rev., 126, 517 (1962).